Review

Graphene Family-Calcium Phosphates for Bone Engineering and Their Biological Properties

Manuri Brahmayya *, ALAPARTHI VENKATESWARA RAO, HAN-TSUNG LIAO *, Jyh-Ping Chen

Posted Date: 7 March 2024

doi: 10.20944/preprints202403.0428.v1

Keywords: Graphene-Calcium phosphate; nanocomposites; osteogenic differentiation; mechanical properties; bone tissue engineering

 doi:10.20944/preprints202403.0428.v1

Review

Graphene Family-Calcium Phosphates for Bone Engineering and Their Biological Properties

Manuri Brahmayya [1,2,*], Alaparthi Venkateswara Rao [3], Han Tsung Liao [1,*] and Jyh-Ping Chen [4]

[1] Department of Plastic and Reconstructive Surgery, Craniofacial Research Center, Chang Gung Memorial Hospital, Chang Gung University, Kwei-San, Taoyuan 333, Taiwan, ROC
[2] Department of H & S, Marri Laxma Reddy Institute of Technology (MLRIT), Dundigal, Hyderabad, Telangana
[3] Department of Physics, KL University, Mangalagiri, Vijayawada, CMRDA, India
[4] Department of Chemical and Materials Engineering, Chang Gung University, Kwei-San, Taoyuan 333, Taiwan
* Correspondence: brahma.orgchem@gmail.com (M.B.); lia01211@gmail.com (H.T.L.)

Abstract: Graphene family (GF)-Calcium phosphate (CaP) composites, holds great potential as components of bone regeneration materials. GF nanomaterials can be modified physically as well as chemically, which are to be biomimetic, mechanically to be hard due to their capability to support exceptional mechanical, thermal and electronic properties. These biocompatible GF composites coated on the calcium phosphate can enhance and tolerate stem cell growth and differentiation, proliferation into various lineages or interact with bioorganisms. The development in CF-CaP materials and their physicochemical/biointeractions and strategies towards osteoblasts is a great concern to promote faster healing and reconstructions of large bone imperfections or defects. In this review, we explain the influence of the CF-CaP and summarize recent developments on designing CF-CaP architectures as multifunctional bone regeneration platforms. We have also explored the typical biological applications concerning these CF-CaP based bioactive nanocomposites. Furthermore, the future viewpoints and evolving challenges will also be emphasized. Due to the shortage of full-length reviews in this emerging research field, this review would be caught great attention and encourage various new chances across a wider range of disciplines.

Keywords: graphene-calcium phosphate; nanocomposites; osteogenic differentiation; mechanical properties; bone tissue engineering

1. Introduction

Bone tissue regeneration is of high attention to upgrade faster healing and restoration of large bone defects formed by skeletal abnormalities, tumor resection, fractures and infection [1]. This review emphasis on graphene family (GF)-calcium phosphate (CaP) (graphene family i.e Graphene (G), Graphene oxide (GO), reduced graphene oxide rGO) based bone substitute materials which can be used for bone repair, bone replacement, regeneration or augmentation [2–8]. GF-CaP biomaterials had paid much attention due to its bioactivity [9,10]. Thus, this review will also contain the effect of the surface structure of calcium phosphate as well as its physicochemical properties after the addition of GF nanomaterials [11,12]. The development of this field needs the utilization of substrates that aid cell connection and differentiation [13–15]. Many diversity materials can stimulate, initiate and tolerate the series of complex actions that can make cell differentiation as well as osteogenesis. In general, collagen can exhibit proper surface chemistry for cell differentiation and cell growth but holds poor mechanical properties and is disposed to immune response [13,16,17]. Hydrogels, which are with tunable physicochemical properties, may positively direct stem cell purpose. Yet, their frontiers may include deficiency of cell-specific bioactivities and it is puzzling to generate bulky structures due to the requirement of a highly bridged network that can affect cell behavior [18–20].

 doi:10.20944/preprints202403.0428.v1

So, materials with significant characteristics needed to survive cell growth and encourage differentiation to hold a boundless potential for stem cell research.

Graphene and its derived products GO and rGO have acknowledged increasing attention for biomedical applications as they can show remarkable properties such as high surface area, high mechanical strength, electrical strength, and an ease of chemical modification [13,21–25]. Graphene is specially framed with sp^2-bonded carbon atoms [26]. In addition, G is the thinnest and most durable monolayer and lightest material and it can exist freely. Individual graphene nano sheets were initially separated from graphite when Scotch tape had been used to peel for preparing graphene include growth from a raw carbon source, cutting open carbon nanotubes, sonication, and reducing carbon dioxide or graphite oxide [27,28]. In addition, GO is an outstanding hydrophilic material by introducing oxygen-containing functions onto the graphene surface, such as hydroxyl, carbonyl, carbonyl, and carboxyl. Owing to its good dispersity in water, high featured ratio and pleased mechanical properties, GO has become a best competitive material to reinforce cementitious materials [29,30]. Lu et al. [31] reported that 0.05 wt. % GO lead to 11.1% and 16.2% rise in flexural strength and compressive strength of the cement paste. Duan et al. [32] demonstrated that 0.03 wt. % GO sheets enhanced the tensile strength and compressive strength of the Portland cement composite by more than 40% as a result of the reduction of the pore structure. Nevertheless, fewer studies examined the outcome of GO on the properties of the magnesium potassium phosphate cement (MKPC) paste [33]. rGO can exhibit powerful factors in helping the spontaneous osteogenic differentiation of osteoprogenitor cells as well as visualizes that the rGO would be the potential candidate for scaffolds in tissue engineering, stem cell (SC) differentiation and constituents of implantable devices, due to its biocompatible and bioactive properties [34]. GF-CaP based nanomaterials showed great interest on osteoinductivity with the Western blotting, immunocytochemistry, and the Alizarin red staining assay with any increased rGO in GF-CaP materials, which is due to the distinct surface properties and chemical properties of GF-CaP.These GO nanomaterials have been also shown interesting optical and magnetic properties, which make them a favorable nanomedicine for diagnostic imaging-mediated therapies [35]. Furthermore, many studies have been enthusiastic to the behavior and toxicology of calcium phosphate coated graphene nanomaterials both in vitro and in vivo [36,37]. Above and beyond, the applications in phototherapy, drug/gene delivery and bioimaging, latest studies have exposed that GF-CaPs architectures can significantly help interfacial interactions with bioorganisms, such as mammalian cells, protein and microbials, which creates them a probable platform for multifunctional biological uses. GF-CaP can enhance the adsorption of extracellular biomolecules, specifically proteins, consequently accelerating the extracellular matrix (ECM). This finally helps cell colonization by providing an extra beneficial microenvironment for cell adhesion and growth. Besides, GF-CaPs can show better network with cocultured cells by physicochemical stimulation, thus affecting their cellular signaling and biological activities, such as electrical stimulated proliferation, differentiation or topography regulation, and stiffness induced stem cell differentiation [10,37–40]. Inspite of there are already a huge number of reports that have been devoted to the investigationof GF-CaP-coated bioactive materials, we noticed that acomprehensive review in this specific field is still lacking. Thereforewe will review the recent developmentsand perspectives for the application of physicochemical interactiveor biointeractive GF-CaPcoatings in biological zones. In this perspective, we will explain bone structure and properties, chemistry and bioorganisms interactionsbetween GF-CaPs including the chemical strategies for developing two-dimensional (2D) and 3D based GF-CaP based surface coatings and thin films for promoting the interface bioactivities. Finally, we will discuss the typical biological applications onthese emerging biomedical applications of GF-CaP coatings.

2. Structural and Chemical Properties of Bone

Bone is a basic unit of the human skeletal structure and functionally graded material with an inner cancellous as well as outer cortical bone. Different loading conditions impact the improvement of macroscopically diverse bone structures in vivo with wisely designing shapes, spatial distributions and mechanical properties [25,41–43] (Figure 1). Bone also provides the framework that bears the

Preprints.org (www.preprints.org) | NOT PEER-REVIEWED | Posted: 7 March 2024 doi:10.20944/preprints202403.0428.v1

weight of the animal body and protects the vital organs, hosts maintain iron homeostasis and hematopoietic cells. Nearly 206 diverse bones make up the skeleton, ranging from the long bones (in our limbs), to smaller bones (In the wrist and ankle) to flat bones (in sternum and skull), to uneven bones such as the vertebrae and pelvis. Bone is a remarkable tissue, a complex composite of biomineral and biopolymer. The biopolymer contains matrix proteins, generally collagen [type 1] with some minor but significant non-collagenous proteins like proteoglycans, osteogenic factors (e.g., bone morphogenetic proteins) and minor amounts of lipids [44]. The non-collagenous proteins and proteoglycans contain a petty total weight of an organic constituent (25%), even though they still having a significant role in tissue mineralization and osteoblast differentiation [45]. The mineral section of bone nearly provides 65% of the bone matrix by its weight (which is primarily in the formulation of calcium hydroxyapatite (HAp)–$Ca_{10}(PO_4)_6(OH)_2$). The bone microenvironment and nanocomposites biocompatibility are convincingly favored when bone repair nanoscale materials are designed [24]. As with all tissues in the body, a bone matrix has a hierarchical organization over length measures that span many orders of magnitude from the macro scale to the nanostructured extracellular matrix (ECM) components (Figure 1). The nanocomposite structure (e.g collagen fibers strengthened by calcium hydroxyapatite crystals) is an integral to the essential compressive reinforcement and high fracture toughness of the bone [46].

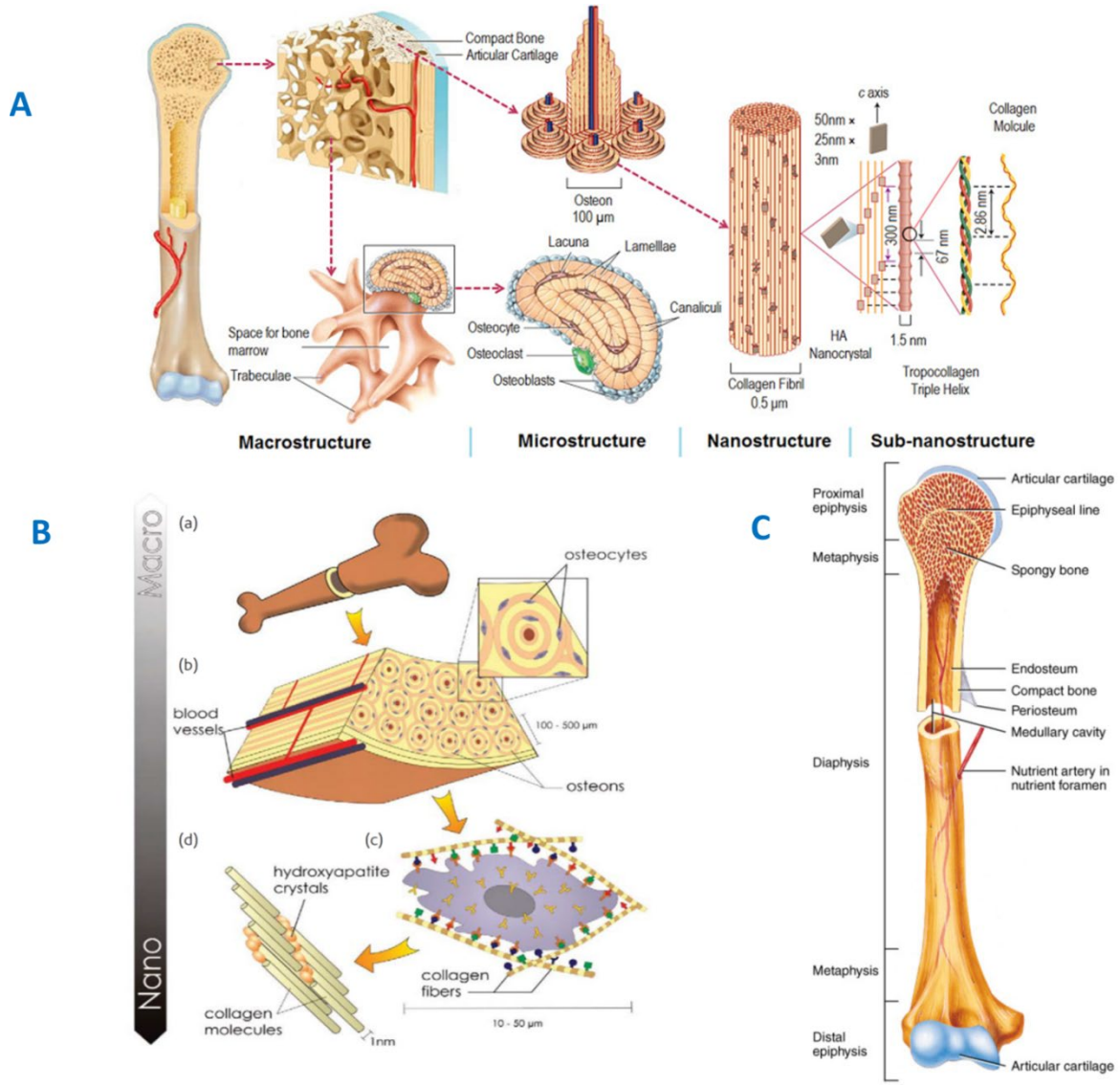

Figure 1. A) Hierarchical structure of bone and bamboo a). In bone, macroscale arrangements involve both compact/cortical bone at the surface and spongy/trabecular bone (foam-like material with ~100-µm-thick struts) in the interior. Compact bone is composed of osteons and Haversian canals, which

 doi:10.20944/preprints202403.0428.v1

surround blood vessels. Osteons have a lamellar structure, with individual lamella consisting of fibres arranged in geometrical patterns. The fibres comprise several mineralized collagen fibrils, composed of collagen protein molecules (tropocollagen) formed from three chains of amino acids and nanocrystals of hydroxyapatite (HA), and linked by an organic phase to form fibril arrays. Reproduced with the permission of nature publishing group@2014. Ref. [116], B) Hierarchical organization of bone over different length scales. Bone has a strong calcified outer compact layer (a), which comprises many cylindrical Haversian systems, or osteons (b). The resident cells are coated in a forest of cell membrane receptors that respond to specific binding sites (c) and the well-defined nanoarchitecture of the surrounding extracellular matrix (d) (Reproduced with permission from56. © 2005 American Society for the Advancement of Science. Ref. [117]. C)Aclear typical structure of long bone. Ref. [9].

In addition, bone in any healthy living organism will adapt to the loads beneath which it is located [47,48]. If loading on the bone increased, it will adjust itselfover time to become stronger by first altering the interior architecture of the trabeculae, later thickening the external cortical portion of the bone. Conversely, if the loading on the bone decreases,then it will become lesser dense due to the lack of the stimulus essential for continued remodeling, where this process regarded as osteopenia. This might be happened, eg.After insertion of an artificial joint due to stress protective that results from the greater rigidity (Young'smodulus of elasticity) of the metal compared to the bone.It is also noteworthy to understand the structural interactions and relationship between the several levels of hierarchical structural organization to know the function of hydroxy apatite within it: (1) the microstructure and sub-microstructure:Haversian canal, osteons, lamellae; (2) themacrostructure: cancellous versus cortical bone; (3) The nanostructure: fibrillar collagen; (4) the sub-nanostructure: molecular constituents of the mineral, collagen, and non-collagenous organic proteins

The microstructure of bone contains mineralized collagen fibers to make it into planar arrangements called lamellae [49,50] (Figure 1a,b). As seen in Figure 1a, in some cortical bone the lamellae wrap in concentric coatingsaround a central canal, to builda osteon (i.e a Harversian system). The osteons usually look like rolls, and they are coarsely parallel to the long axis of the bone [50]. The other arrangements of corticalbone in which no such kind pattern can be distinguished are called the woven bone while the microstructure of trabecular bone has a dissimilar arrangement. It resembles a fiber texture,where all the mineral platelets are organized parallel to a common direction which is resultant to the fibredirection of the collagen. This common direction shows some spreading and it is defined approximatelywithin $\pm 30^{o}$ [51].

On the macroscopic stage, bones can have varied forms depending on their respective purpose [51]. See Figure 1c Cortical bone produces the outer shell of bones. It is a properly dense bone, with the porosity [49–51] in theorder of 6%. On the other hand, the other type cancellous bone forms inside of bones that isunderneath compressive stress.The interrelating framework of trabeculae is in a several numbers of combinations, in which all are following basiccellular structures: rod-rod, rod-plate, or plate-plate [50–54]. In case of the trabecular bone, it is having pores in the order of 80% [55] and the typical thickness is about 50–300 μm which depends on the load distribution in the bone with respect to the orientation [56]. When directing in vivo study of osseointegration of coated and uncoated implants, one should consider into an account the reactivity of bone surrounding the implant.Namely, at the diaphysis (Figure 1c), native bone is in neighboring contact with an implant. The metaphysis(Figure 1c), on the other hand, it consists cancellous bone which is more reactive and hence it provides faster facture healing [57].

In the lamellae's nanostructure, there is a mineralized collagen fibril, which is about 100 nm in diameter. The fibrils contain an assembly of 300 nm long and 1.5 nm dense (thick) collagen molecules. The collagen-I is the key organic component of the matrix. The collagen molecules are secreted by osteoblasts, and which are then self-assembled. Apatite crystals come about within the distinct spaces in the collagen fibrils. Additionally, the collagen in the fibrils also limits the probable primary growth of the crystals, driving them to be discrete and discontinuous. Crystals gained at regular intervals beside the fibrils, with a roughly repeated distance of 67 nm [58,59], which agree to the distance by

 doi:10.20944/preprints202403.0428.v1

which neighboring collagen molecules are staggered. It is thus significant to notice that the arrangement of the lamellae and collagen fibres up to the nanoscale increase the isotropic assets found in bone hinder,the crack proliferation, and enhances robustness [58].

The generation of the apatite in the extracellular region of the collagen is called biomineralization. It is also most important to note that the procedure varies depending on various factors such as situation of the stage, region, and age of the particular bone. The nucleation procedure in the bones is allied with interaction among anionic proteins and type I collagen fibrils which may provide the stereochemical alignment of negatively charged functions that is adequate for hydroxyapatite nucleation. When the bone matrix is generated, a representative time course of nearly 2 weeks will take place before the matrix initiates to mineralize speedily. This mode is called primary mineralization, and within a few days, the matrix can be mineralized up to 70%. The residual 30% of enhancement in mineral content lasts numerous years, and is called secondary mineralization [60]. Epitaxial concerns have been found to be of primary significance in biomineralization, in apprehension the generation of teeth and bones, as well as in pathological ways such as the progress of urinary calculi [50–59,61].

With reference to the structure of bone mineral crystals, the major studies revealed them as plate-like in structural shape [The thickness of the platelets is between 1.5 to 9 nm, while the length is about 15-200 nm, and the width is about 10-120 nm [62–70]. The shape and size of bone apatite crystals vary with age, species and disease state. For bone mineralization process in a specified species, the averagesize of the crystal is minimal at generation and enhances to maturity and there is levelling of this growth procedure at given time. Additionally, a single specimen covers a range of particle shapes and sizes, and various measurement methods may yield dissimilar average standards on polydisperse models [71]. The circumstances in the human being body apparently permit limited growth of hydroxyapatite in vivo. The better effective inhibitors seem to be polyanions, polyphosphonates orpredominantly polyphosphates. Salivary proteins and peptides, such as praline-rich proteins (PRPs) and statherin, are powerful inhibitors. This macromolecule seems to stop the precipitation of calcium phosphate (CaP) phases in saliva despite the supersaturation of this specific secretion with regard to HAp. The mechanism of this inhibition was allied to their adsorption on surface of apatite sources [72–75]. However, proteoglycans at low concentrations can prevent or delay apatite generation. Conversely, the bone collagen has been considered to be involved in the nucleation of inorganic mineral (i.e bone mineral) [76–78].

There was a limited knowledge of the crystal structure of biological apatites due to the absence of proper single crystals for study [79–81]. However, it was described that the isolated crystals as ofthe natural bones were weekly crystalline apatite, alike to powdered intact bone where they were initiated [82]. There are two different kinds of crystallographic structures had been suggested for biological apatites [83–85]: (1) hexagonal and (2) monoclinic with lattice. These both structures could share the same elements calcium and phosphorus with the stoichiometric ratio Ca/P of 1.67. The maindissimilarity between them is the positioning of the hydroxyl functions. In the hexagonal hydroxy apatite, two nearby hydroxyl functions point at the opposite direction, whereas in the monoclinic form—hydroxyl functions have the same direction in the same column, and a reverse direction among the columns [86].

In the view of the chemical composition of bone, the biological apatites differ from thestoichiometric composition of hydroxyapatite, $Ca_{10}(PO_4)_6(OH)_2$ and consist important amounts of several necessary ions such as Mg^{2+}, Na^{+}, K^{+}, citrate, HPO_4^{2-}, carbonate, Chloride, Fluoride ions [87–90], etc. Aqueous biological fluids, these substitute ions changes over time by each and others [91,92]. Some analysis like FT-IR (Fourier Transform Infrared Spectroscopy) on the bone mineral reveals that the nanocrystalline apatite is covered with a hydroxy layer covering ions, such as Ca^{2+}, HPO_4^{2-}, CO_3^{2-}, in dissimilar sites of the crystal, which can be considered as dibasic calcium phosphate dehydrate phase ($CaHPO_4.2H_2O$) or octacalcium phosphate $Ca_8(HPO_4)_2(PO_4)_4.5H_2O$ phase [93,94].In several literature reports, the Ca/P atom ratio of biological apatite was either close or lower than that of stoichiometric Ca/P = 1.67 [87,95–97]. Nevertheless,Ca/P > 1.67 has been defined too [98–100]. The exclusive chemical composition of biologicalapatite is exposed by: (a) the lack of anticipatory

 doi:10.20944/preprints202403.0428.v1

hydroxyl function, and (b) the existence of HPO_4 [2–101].For hydroxyl group, it was stated that only a few percentages of anticipated concentration was noticed in bone [102–104]. The existence of HPO_4^{2-} is attributed to either ionic exchange, or to hydrolysisof PO_4^{3-}.

On further, bone has four major kinds of cells: a) osteoblasts b) osteocytes c) osteoclasts, and d) bone lining cells. Generally, osteoblasts are bone developing cells. They are initiating from the osteogenic cells differentiation in the tissue whichthen covers the bone marrow. The preparation of bone matrix by osteoblasts takes place in a couple of steps such as a deposition of organic matrix and then its subsequent mineralization [105–107]. When the osteoblast is completed working, it is thus actually confined inside of the bone after it hardens. This particular stage is known as an osteocyte. Therefore, osteocytes are well developed bone cells and act as stress sensors in the bone matrix. The osteoblasts whichstill remain on the top of the new bone and were used to defend the underlying bone, these are known as lining cells. These lining cells help the bone without interfering with other cells functions. Osteoclasts are big multinucleate cells which areaccountable for the collapse of bones. Bone is a complex material wherein CaP is accountable for the hardness, rigidity, mechanical and high resistance to compression [108–120].

3. GF-CaP: Bioorganisms Interactions

3.1. GF and GF-CaP Coatings: Chemistry

In general, graphene oxide was prepared from graphite via two primary methods: (a) top-down method or (b) bottom-up manner. The most common top-down method is Hummer's procedure which could generate a facile protocol for the production of oxidized graphenenano sheets with a better solution process-capacity. Many modified Hummer's methods were developed for the past several decades to produce various nano size shapes or layers with an oxygenated contents [121–126] Figure 2. The common procedure of Hummers' process can be concluded as showed in and in which the graphite in a flake, powder or block form will be chemically exfoliated or oxidized into a nano layered structure, with an assistance of sonication, single or multi-layer oxidized graphene (Called as GO) could be obtained [123–128].This technique was also further modified by electrochemical exfoliation of graphite via applying an external electric field; it was regarded as a production of high-quality graphene oxide with fewer defects only in most of the Hummer's techniques [Figure 2b].Graphene was also synthesized from chemical vapor deposition (CVD) method [Figure 2c] and regarded as another representative top-down method, in this procedure, large graphene sheet with diverse sizes and layers can be achieved by applying copper alloy and silicon carbide as substrates [129,130]. Due to high conductivity and the fine structure, the CVD prepared graphene has been measured as the prime method for the production of graphene-based electronic devices. On the other hand, in the bottom-up production of graphene, one of the most thrilling methods is described by the research groups like Fasel and Mullen. These groups reported that atomically accurate graphene nanomaterials (GNMs) with various widths, edge periphery and topologies can be manufactured via surface-assisted polymerization and cyclodehydrogenation of specific precursors [131]. They also reported that the similar bottom-up technique can be applied for the preparation of zigzag graphene nanomaterials (GNMs) with yielded atomically exact zigzag edges [132,133].

Preprints.org (www.preprints.org) | NOT PEER-REVIEWED | Posted: 7 March 2024 doi:10.20944/preprints202403.0428.v1

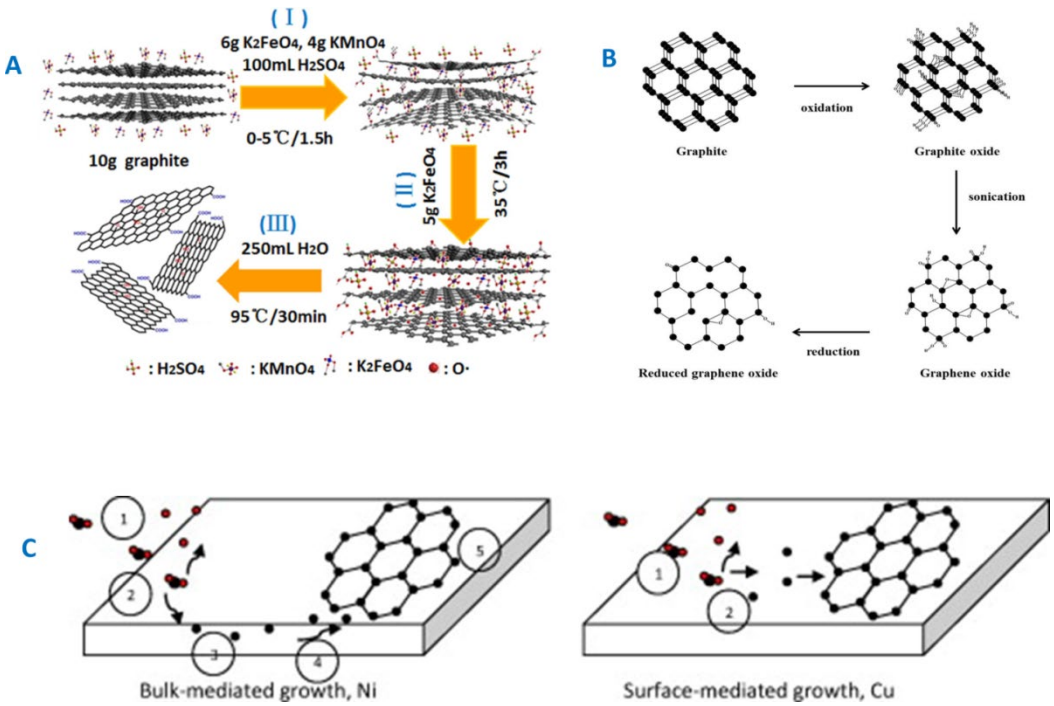

Figure 2. A) Illustration of the preparation of GO based on an newly improved Hummers method. Ref. [118] B) 11. Schematic images of the process used to produce reduced graphene oxide (rGO). Ref. [9]. C)Reproduced with permission of Elsevier copyright @2014. Ref. [119].

From the observation of graphene material's chemical and physical properties, it can be divided into three types: (a) pristine graphene (b) graphene oxide (c) reduced graphene oxide. Pristine graphene is a thin layer of pure carbon i.e graphene produced by CVD via the exfoliation of graphite [134]. Since these CVD derived graphene materials are having fine aromatic structural properties with a lower number of defects, Figure 4., these graphene nanosheets are problematic to suspend in solutions and consequently not advantageous to use them as nanocarriers or nanomedicine. Conversely, their highly reactive edge surfaces make them feasibly fit for bioelectrodes, for an occasion, the detection of chemical molecules and to bioorganisms.GO is a hydrophilic oxidized structure of graphene or graphene layer has oxygen groups i.e carboxyl, epoxy and abundant hydroxyl groups, especially on its edges and defects as well as hydrophobic sp^2- and sp^3- bonded carbon atoms, hence bring into being a sheet-like amphiphilic colloid [135].

GO can steadily suspend as amphiphilic colloids in an aqueous and many polar solvents through its hydrophilic groups. Because of the rich residual sp^2-bonded carbon environment on the GO basal plane, GO is gifted of π-π interactions with aromatic moieties. The polar functions, epoxide, hydroxyl and carboxyl acid, on basal plane allow GO to undergo weak or strong interactions with other substrate or organisms depends on their physical and chemical properties [136].Reduced graphene oxide (rGO), (Figure 2A,B) can be achieved by reduction of GO with several chemical, thermal and irradiation approaches. When compared to graphene or graphene oxide, rGO has abundant balanced physical and chemical properties, concerning to solvent dispersibility, thermal, surface chemical groups, optical, mechanical, and electrical performances [137]. Based on the above facts of GF, several people prepared inorganic-based nanocomposites to improve the osteoinductive effect on hMSCs.Various techniques [9,12] could be explored to make these interesting materials (GF-CaP), which are summarized in (Table1). In several cases, GF-CaP biomaterials prepared in high temperature or high pressures have mechanical properties and high crystallinity, such as synthesis, spark plasma sintering and hot isostatic sintering. Nevertheless, thermal spraying methods typically lower the crystallinity of the HAp coating. HAp could be blended onto graphene and its derivatives and directly mixed together with the nanofillers by ball milling and ultrasonic dispersion.

 doi:10.20944/preprints202403.0428.v1

Table 1. Various approaches of the GF-CaP related coatings [2,9,12,40,138–165].

Technology	Categorized procedures	advantages	ref
Synthesis	To synthesize rGO-coated BCP graft material, as-prepared rGO in water was sonicated for 2h, and then mixed with BCP suspended in deionized water at rGO toBCP with various weight ratios. The rGO-coated BCP graft material got by vigorously mixing colloidal dispersions of rGO nanoplatelets and BCP microparticles for few minutes only (Approximately 10 min) andat room temperature overnight. & Graphene nanoplatelets were used as the toughening agent. For BCP, first, CDA nanopowderswere prepared bychemical precipitationofCa(NO_3)$_2$ and (NH_4)$_2$$HPO_4$ with an appropriate Ca/Pratio.Then,BCPnano powders,amixtureof70wt% HA and30wt% β-TCP were collectedaftercalcininghe obtained CDAat550 ^{0}C. GNPs weredispersed incetyltrimethylammoniumbromide (CTAB) solutionbysonicationfor 1h.Thenthesuspension and BCPnanopowdersweremixedbyballmillingfor8h. After beingdried,suchmixturesweretreatedat500 ^{0}C for1h in argontoremovethesurfactant. Eventually,thecomposites were fabricated byhotpressingthescreenedpowdersat 1150 ^{0}C inamultipurposehightemperature furnace under a pressureof30MPain an argonatmosphere for1h.ThecontentsofGNPsinthe compositeswere0,0.5,1.0,1.5,2.0and2.5wt%.	It is a nontoxic and stable bone graft material. It can increase the bone regeneration better than BCP alone. GNPs/BCP composite are promising bone substitute materials as well as effective additive for toughening ceramics for bone substituents.	[9,12]
Electrochemical Deposition	a) The dispersion of graphene is dripped on copper electrode and carbon film on copper grid by polyethylene terephthalate (PET) dropper, and then dried by air blower. & b) The electro-deposition was carried out on a two-electrode system with a stable cathodic potential of -4.0 V at room temperature.	The electro-deposition procedure is a facile, environmental friendly and controllable route towards the synthesis of promising graphene-CaP composite for biomedical applications.	[2,138–140]
Spark plasma sintering processing	Graphite papers were placed between pure HA, 0.5 wt.% graphene nano sheets (GNS)/HA and 1.0 wt.% and die/punches for easy specimen elimination, using a maximum temperature of 1150 ^{0}C and a holding pressure of 40 MPa. A	It is expected that (GNS)/HA could provide more desirable locations for osteoblast adhesion, as well as	[141–144]

 doi:10.20944/preprints202403.0428.v1

	heating rate of 150 ^{0}C/min was applied until 1050 ^{0}C was reached, with 1150 ^{0}C being attained in the next minute; this maximum temperature was kept for 3 min. The samples were then furnace cooled to ambient temperature.	creates more nucleation sites enabling apatite mineralization.	
Electro spinning	The graphene/HA mixture in organic solution and then subjected to high voltage and being subjected out from the spinnerret	High porosity and connectivity	[145–147]
Self-assembling	Dispersing the graphene oxide/HA into aqueous solution	Controllable porosity and connectivity and good mechanical strength	[148,149]
Thermal Spray	Graphene into the aqueous solution, HA preparation using wet chemical synthesis, spray coated onto the substrate material	Controllable coating thickness and large area deposition and strong adhesion feature	150
3D printing	Dispersion of graphene/HA into the specific organic liquid or using 3D printer to synthesize 3d scaffold.	Controllable porosity and connectivity	[151,152]
Chemical vapor deposition	Au nano particles or clusters are dispersed over HA particles and acetylene and methane are the carbon source using radio frequency chemical vapor deposition	High graphene purity and large graphene sheets	[153,154]
Hot isostatic pressing	Mixing graphene and HA using mechanical milling / ultrasonic dispersion and sintering at high temperatures under high pressures	Ultrafine microstructures, high HA crystallinity and holding fine grain shapes and sizes	[155–158]
Biomimitic mineralization	Graphene family powdered substances were decorated by bioactive materials	Increased osteogenic activities with bone like apatite production	[159–165]

In synthesis, rGO-coated BCP graft material was prepared using the BCP microparticles i.e mixture of HAp and β-TCP (3:7 by weight). The readily prepared rGO in DI water was subjected sonication for 2h, and then mixed together with BCP, suspended in DI water at rGO to the BCP weight ratios of 2:1000, 4:1000 and 10:1000. The rGO-coated BCP material was gained by robustly mixing colloidal diffusions of rGO and BCP microparticles for a while (10 min) and was slow air-dried at RT for overnight [9]. Nano HAp particles are effectively fabricated on GO [10,12], chitosan modified [12] GO and rGO surfaces [9] using in situ synthesis approaches. Generally, as shown in Figure 3, GF based powders [12] are initially dissolved and exfoliated in deionized (DI) water by sonication to attain a uniform mixture; later $Ca(NO_3)_2$ is added into the GF based solutions by stirring for a preferred time; subsequently, the pH of the suspension is changed to 9-10 using ammonia solution,

Preprints.org (www.preprints.org) | NOT PEER-REVIEWED | Posted: 7 March 2024 doi:10.20944/preprints202403.0428.v1

and $(NH_4)_2HPO_4$ was added into the mixture [12]]. The SEM and TEM images of the physicochemical characteristics of rGO/HAp shown in the Figure 4.

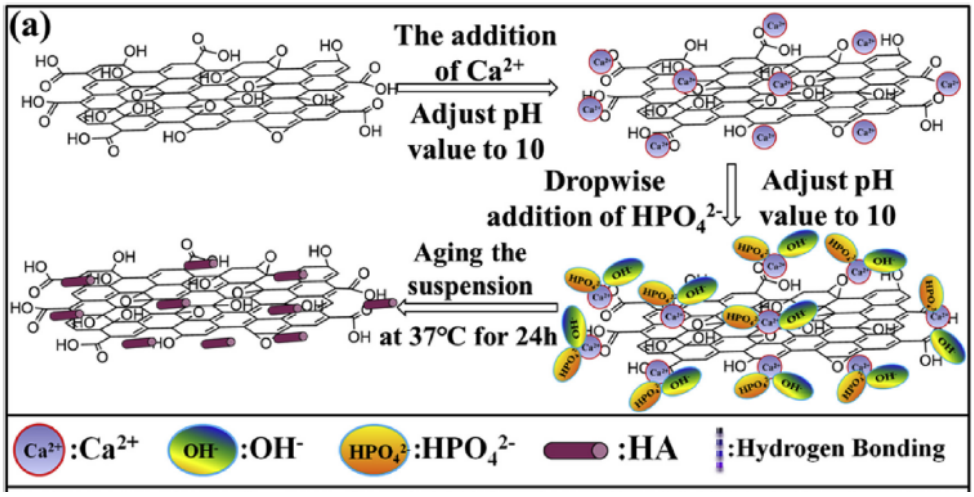

Figure 3. The proposed in situ synthesis mechanism of HA on pristine GO sheets. Ref. [12]. Reproduced with the permission of Royal Society of chemistry@copyright 2012.

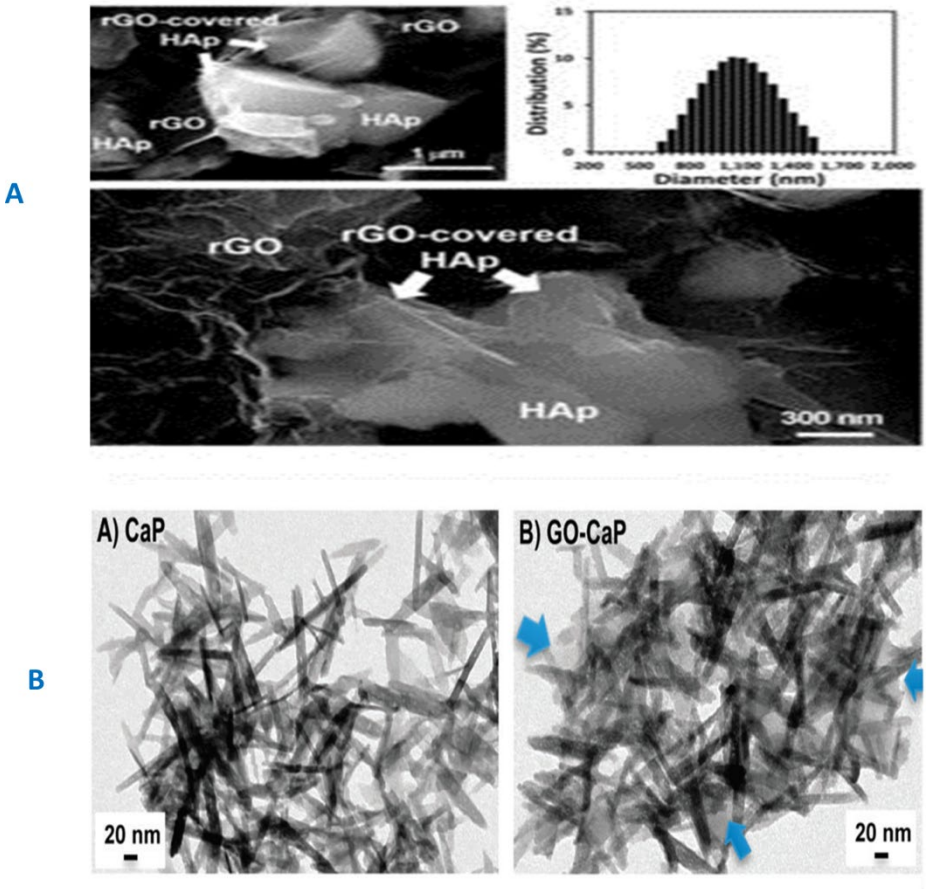

Figure 4. A) FESEM images of the rGO/HAp NCs show that the morphology of the HAp MPs was irregular-shaped granules with a mean particle size of 960 } 300 nm as well as that HAp MPs were partly covered and interconnected by an network of rGO NSs. Ref. [10], B) TEM images of mature (A) CaP nanoparticles and (B) GO–CaP nanocomposites at 2 weeks after fabrication. Blue arrows on (B) point to the edge of underlying GO sheet. Scale bars indicate 20 nm. Ref. [167].

Preprints.org (www.preprints.org) | NOT PEER-REVIEWED | Posted: 7 March 2024 doi:10.20944/preprints202403.0428.v1

The subsequentcompound solutions are suggested to be aged for days to confirm the fully transformed apatite into hydroxyapatite with worthy phase purity as well as crystallinity. For the duration of the synthesis, the oxygen-containing functions on the GO surfaces act as receptor sites for Ca^{2+}via electrostatic interactions; where these anchored Ca^{2+}can in situ react with phosphate ions to get apatite nanoparticles. The essential reaction mechanism has been suggested by Li et al. [12]; the spreading and the microstructures of HA on graphene are mostlyaffected the amounts and categories of the oxygen functions on the GF based templates and the concentration of the reagents ($Ca^{2+}$and HPO_4^{2-}), solution pH ranges and so on.

In an electrochemical deposition, HApwas involved in dissolving calcium/phosphate ions in a buffer solution with organized pH values and temperature underneathchanging electrical current [138].Once the voltage is applied, Ca^{2+}will transfer to the surface of cathode due to electrostatic attraction and react with the OH^- therein generated by the electrolysis of water, subsequently in the in situ nucleation and growing of HAp on the surface of cathode [139]. Zeng et al. [140] fabricate GO/HApsurface coatings on Ti via this technique; GO was distributed and mixed with the electrolyte for deposition which containsCa $(NO_3)_2$, $NaNO_3$, $NH_4H_2PO_4$, and H_2O_2. The occasioning pure HA coating shows an irregular morphology with shell-like flakes, and the GO/HA complex coating displaysunbroken and porous topography. The upsurge of GO fillings in the electrolyte can increase the HAp crystallinity as well as the bonding strength of the coatings. On the other hand, the applications of HAp for hard tissue grafts are inadequate by the low mechanical strength of associated HAp [141]. Throughout the conventional sintering procedure, HAp will separate into tri and tetra calcium phosphates at 1000 °C-1300 °C, and generally, the higher temperatures and long sintering time can reason grain coarsening performance, which may depreciate the mechanical properties [141] of HAp. As the othertechnique, spark plasma sintering is an activemethod for making novel nanoceramics at lower temperatures for tiny periods of time, with the benefits of recollecting fine particle sizes. Graphene/HApnano composites are effectively fabricated by spark plasma sintering. The initial powders that are used for spark plasma sintering can be synthesized by mixing HAp powders/nanoparticles and GF sheets together using a mechanical milling [142], sonication [143,144] and prepared by a liquid precipitation way [145]. Different micrometer diameters of graphene are homogeneously dispersed and surrounded within the HAp matrix and situated between the HAp crystal particle boundaries without agglomerations.Characteristic SEMimages of the spark plasma sinteringsamples [9,144]were shown Figure 5.

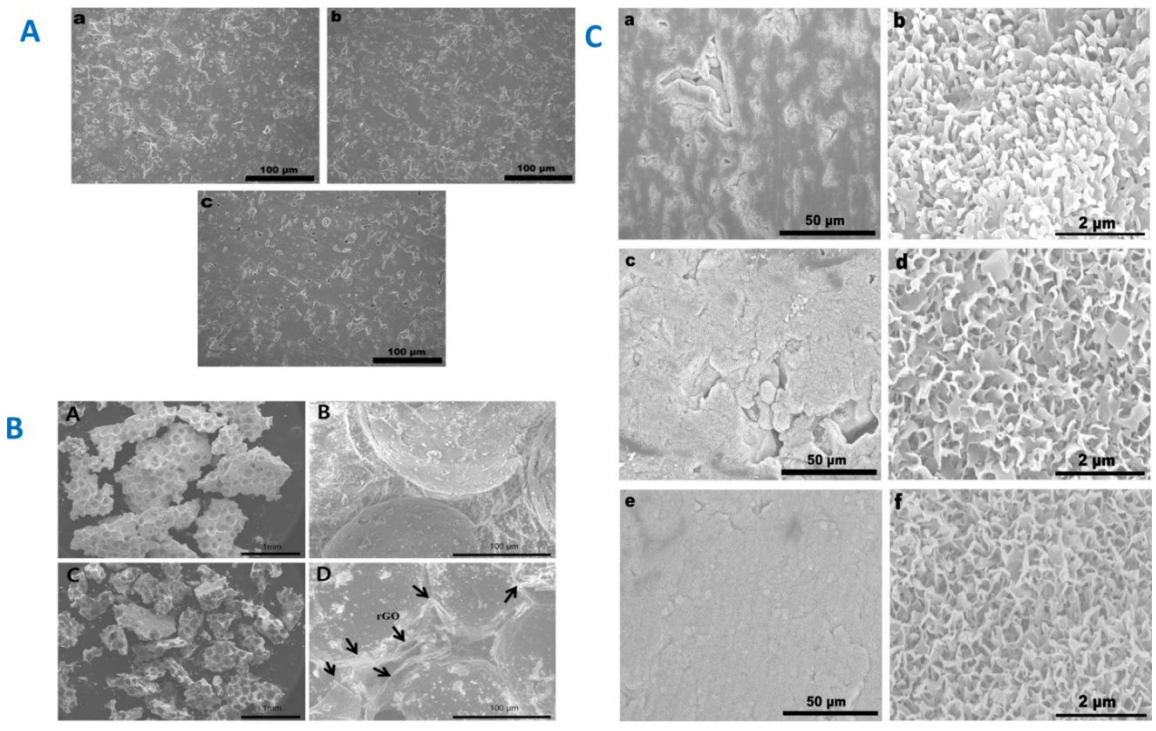

 doi:10.20944/preprints202403.0428.v1

Figure 5. A) SEM images of the surfaces of (a) HA, (b) 0.5 wt.% GNS/HA composite and (c) 1.0 wt.% GNS/HA composite. Reproduced with the permission of Elsevier copyright@2013. Ref. [144]. B) Field emission scanning electron microscope (FE-SEM) images of biphasic calcium phosphate (BCP) microparticles (magnification: 30x (A); 500x (B)) and reduced grapheneoxide (rGO-coated BCP bone graft materials (magnification;:30 x(C); 500x(D)). Arrow s indicate the rGO nanoplatelets. Ref. [9]. C) Low- and high-magnification SEM images of apatite formation on HA (a and b), 0.5 wt.% GNS/HA composite (c and d) and 1.0 wt.% GNS/HA composite (e and f) immersed in SBF for 7 days, Reproduced with the permission of Elsevier copyright@2013. Ref. [144].

In the electrospinning technique, electrospinning pays an electrical field formed under high voltage to force out the polymeric liquid from the spinneret, causing in a polymeric fibrous and porous scaffolds on the collectors [145]. Ma et al. [146,147] prepared a porous polylactic acid (PLA)/HAp/GO scaffold by using electrospinning technique and SEM images of the composite material were shown Figure 6. In a self-assembling technique, GO offers a facile and effectiveprocess to produce GF-based macrostructures. As shown in Figure 7A, grapheneoxide and HAp nanoparticles (nHAp) mixed together were sonically in ice bath which results in a homogeneous suspension, and later the mixture was heated at 200 °C for 3 h to prompt self-assembly [148]. This method has reducedthe grapheneoxide to rGO without using any reductant substance and organic solvent, which could extremely decrease the cytotoxicity of the composite. The SEM morphology images and the EDS data clearly differentiated the substrate and desired final material (Figure 7).The SEM images (Figure 7A), revealed that the displayed scaffold was porous structure (diameter in range of 20–100 μm). It was also evidently observed that the amplified mass ratio of nHA could alter the morphology of scaffold. Thus, the mass ratio of nHA to GO was a significant parameter affecting scaffold assembly and should be well determined to ensure the good biocompatibility for bone defect repair [148]. The spot EDS analysis (Figure 7B) on SEM images presented that the amount of carbon element on the surface of scaffold reduced with the rise of nHA ratio, indicating that nHA was integrated on the surface of graphene nano sheets [148]. Thermal sprayed HAp and HAp-based coatings have been fruitfully used on commercially accessible Ti-based orthopedic grafts, having the benefit of high deposition rate, decent bonding strength and adjustable coating thickness [149]. This procedure contains, heating the HA powders to melting stage at high temperature, which may reason for the breakdown of HA and show detrimental properties on the coating biocompatibilities. Consequently, other reports [150] alteredvacuum cold spraying as a substitute to prepare GF/ HAp nanostructured coatings at RT [150]. The GF/ HAp powder material is made by wet chemical method, and the sprayed coatings have a measurable thickness and showmodestpasty strength and fracture toughness, with graphene uniformly embedded in HAp matrix [150]. The FESEM and TEM images of the coating [150] were shown in Figure 8.Three dimensional (3D) printing is a greater additive manufacturing system to print scaffold with tailored shape, precise chemistry and porosities and displays great potential for its application in bone tissue biomedical engineering [151]. Even though bone has self-healing capabilities, the heavy bone loss or injury cannot be restored totally and naturally. A matrix or scaffold materials should be incorporated to support this healing course. Ch.Wu et al. [152] manufactured GO surface modified β-tricalcium phosphate (β-TCP) frameworks by,first using 3D printingtechnique and then soaked the β-TCP framework into GO/water suspension for the developments of in vivo osteogenesis.

Preprints.org (www.preprints.org) | NOT PEER-REVIEWED | Posted: 7 March 2024 doi:10.20944/preprints202403.0428.v1

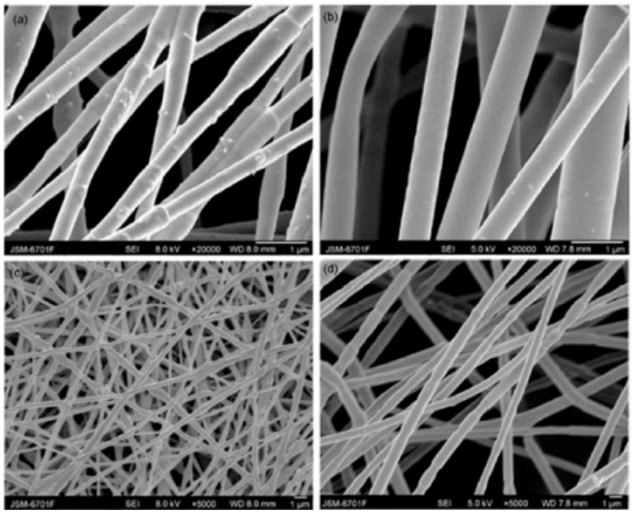

Figure 6. SEM images of PLA/HA/GO nanofibers with high magnification (a) and low magnification (c), electrospun PLA with high magnification (b) and low magnification (d). Ref. [146].

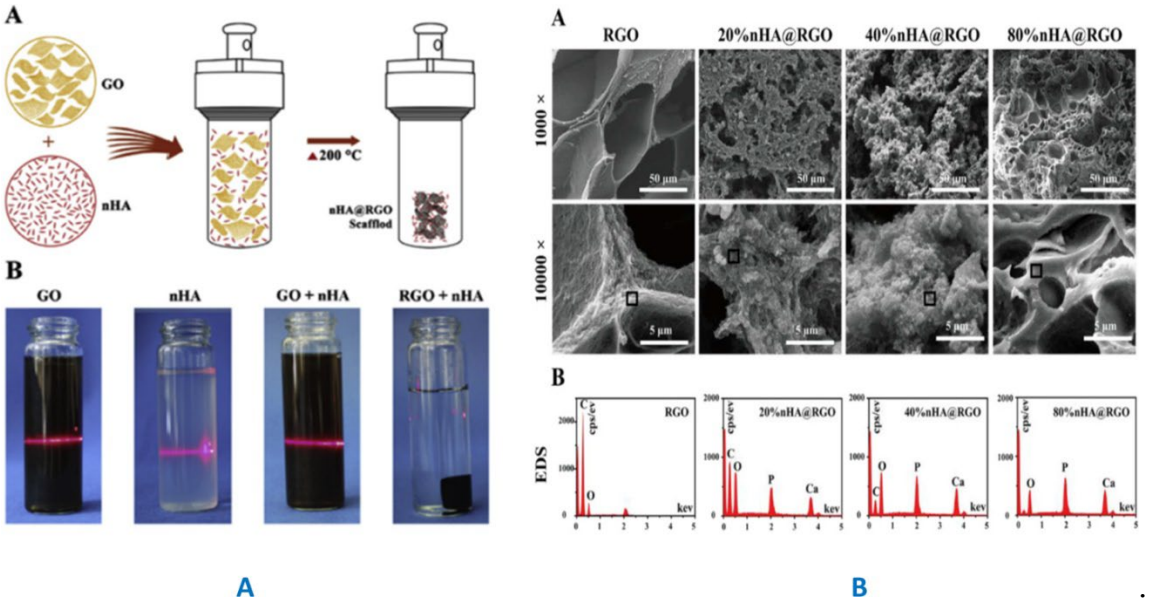

Figure 7. A) (A) Schematic showing that the self-assembly of RGO and nHA to form a porous RGO scaffold for cranial bone defect reconstruction; (B) Tyndall effect of before and after reaction. B. (A) SEM and (B) EDS analysis of the nHA@RGO scaffold with the different nHA loading ratios, the black box on the photo was the sampling area of the EDS.Reproduced with the permission of Elsvier copyright@2017. Ref. [148].

 doi:10.20944/preprints202403.0428.v1

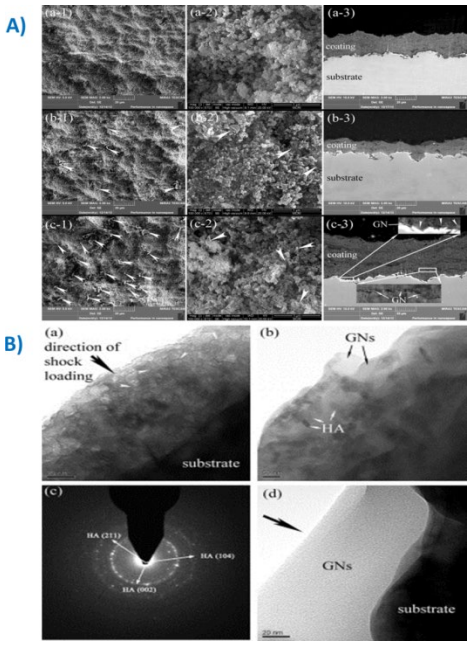

Figure 8. A)FESEM views of the as-deposited nanostructured coatings, (a) the pure HA coating, (b) the HA-0.1 wt.%GN coating, and (c) the HA-1.0 wt%GN coating. -1: surface view, -2: magnified surface view, and -3: cross-sectional view. The white arrow head points to GN located on the surfaces of the coatings, and magnified views of typical areas from the cross-section of the HA–GN coating showing clearly the presence of GN in the coating and at the coating/substrate interface (c-3). GN-induced layered structure is clearly seen for the HA–GN coatings. Permission obtianed with the Elsevier copy right@2014. Ref. [150]. **B)** TEM images of the HA-1.0 wt.%GN coatings, (a) the image acquired at HA-rich area shows dense structure and plastic deformation of certain amount of the nano HA particles at their surrounding part of contact, (b) both GN and HA are clearly seen with intact structure as compared to the starting feedstock, and this is further verified by SAD pattern shown in (c), and (d) TEM image taken at coating/ substrate interface suggests intimate contact of GN with the substrate. Permission obtianed with the Elsevier copy right@2014. Ref. [150].

Chemical vapor deposition is a cost-effective and scalable performance to prepare GF films [153]. Novel biocompatible and multicomponent graphene/HA/Au nanomaterials are prepared by using radio-frequency chemical vapor deposition, with methane and acetyleneas the carbon sources [154]. Throughout the deposition procedure, Au nanoclusters are consistentlyspread over HAp particles with diameters of 2 nm to 7 nm and behave as catalyst for graphene manufacture [154]. This research specifies that longer radio-frequency chemical vapor deposition time can conclude in few-layers graphene with greater [154].

Hot isostatic pressing is a common method to densify presintered constituents, consolidate powders and increase interfacial bonding [155]. It can be demoralized to make HAp ceramics with ultrafine microstructures and knowingly better mechanical possessions [155]. In recent times, graphene is familiarized into this classification as an operative additive for toughening ceramics composites; Novel graphene/nickel-doped biphasic calcium phosphate composite [156], graphene/biphasic calcium phosphate complex [157], and rGO/nanotube HAp composite [158] have been effectively designed by using hot isostatic pressing technique.

Biomimetic mineralization is an environmental benign technique to prepare bone-like apatite underneath ambient conditions in aqueous locations. Generally, GFs are dipped in an unstable or supersaturated solution with calcium and phosphate ions their concentrations parallel to replicated physiological condition, and apatite was driven as nucleated and precipitate on the surface of those GF-based biomaterials. In the process of mineralization, GO greatly enrich the nucleation and crystallization of HAp, resulting in hybrid uniform GO/HAp coatings with densify fine flake-like HAp nanocrystalline [159]. Typically, GFs are surface modified by bioactive materials to provide the

 doi:10.20944/preprints202403.0428.v1

complex with new properties and assist the biomimetic deposition of HAp. The GO can be altered by gelatin to mimic the electrifying proteins in an extracellular matrix (ECM) for a modifiable bone generation, and the existence of gelatin develops the attraction of calcium ions and encourages the nucleation of HAp [160]. As well, GO can also biofunctionalizedby polydopamine [161], carrageenan [162], chitosan [163,164] and fibrinogen [165] to increase the mineralization route. Table 1 show, the most usually used biomaterial composites, nano HAp particles, synthetic polymers and nanoparticles that have been used to get the GF-CaP with worthy biocompatibility and useful biofunctionality. Due to the diverse and exceptional physicochemical and biological properties of GF-CaP, it is supposedto suggest that they can displayplentifuldetailed interactions with tissues, for an example the GF-CaPcombined interface can deliver a more promising microenvironment for cell proliferation and attachment.

3.2. GF-CaP Biointeractions and Effects

Understanding the effect of GF-CaP composites on GF-CaP–cell interaction is essential for considering GF-CaP as a potential candidate for bone tissue engineering [9]. Due to the large specific surface area, good obtainability of functional chemical groups, and exceptional interface properties, the GF-CaP possess extremely great dimensions for bimolecular interactions in evaluation to various other nanomaterials. Recently, biocompatibility of few layers of GF films conveyed to various substrates was evaluated using osteoblasts [166]. The substrates were oxidized soda lime glass, silicon wafer (SiO_2/Si stack) and stainless steel. Chemical vapor deposition technique was employed to produce GFs on a copper substrate by using hydrogen and methane as precursors [166]. The thickness and quality of GF films on dissimilar substrates were assessed by Raman spectra, while the thickness of GF film was defined by reflectance and transmittance spectroscopy. These studies were also focused on cell attachment as well as morphology and shown that graphene does not have any kind of toxic effect on osteoblasts [166]. The cell adhesion increases with graphene coated material rather than the substrate alone [9,166]. It appears that GF properties play a leading role in cell adhesion. This study also suggests that layers of GF on bone grafts will be useful for osteoblast attachment and proliferation. Bi et al. have described that the grapheneoxide-calcium phosphate (GO-CaP) nanocomposites notably helped the osteogenesis of hMSCs with enhanced deposition of calcium, which assists their hopeful future in bone repair [167]. For the bone defect repair, S. Wang et al. reported a α-tricalcium phosphate (α-TCP) based reduced graphene oxide carbon nanotube cement recently and in which rGO could increase the mechanical assets of calcium phosphate cement effectively with the addition of 0–1 wt% [168]. Chengtie Wu et al. prepared that GO-blended β-tricalcium phosphate (β-TCP) biomaterials and proved it in the enhanced osteogenic ability of human bone marrow stromal cells (hBMSCs) instead of pure β-TCP samples both in vitro and in vivo [152]. These scaffolds suggestively improved the activity of alkaline phosphatase, growth and osteogenic gene behaviour compared to the bare β-TCP. The rGO hybridized HAp composites also displayed greater osteogenic differentiation for hMSCs [34]. Jong Ho Lee et al. demonstrated that rGO-hydroxyapatite composites by adding the 1:1 weight ratio of colloidal dispersion nano particles of rGO with suspended hydroxyapatite (water soluble calcium phosphate) microparticles in DI water, which was enhanced the osteogenic differentiation of hMSCs, when incubated in basal media without any osteoinductive agents [10,34]. In addition the above mentioned nano-sized, functionalized graphene (surface-coated) derivatives, GF coated nanomaterials can also exhibit physicochemical properties as graphene or GO in several ways i.e good biocompatibility, versatile biofunctionality, due to the distinctive and extraordinary specific surface area of 2D planar nanosheet structure, great availability of surface functions, electrical conductivity and mechanical properties [152]. Owing to the diverse and excellent physicochemical and biological properties of GF-coated nanomaterials, it is believed that they can exhibit abundant error-free interactions with proteins, human cells, bacterial and tissues, for instance, the GF-CaP interface can offer a more promising and favorable microenvironment for cell attachment and proliferation. Thus, it is of great prominence to understand these irreplaceable interactions with bioorganisms like stem cells and microbials while we study the biological applications of GF-CaP nanomaterial architectures on bone repair research.

 doi:10.20944/preprints202403.0428.v1

Y.C. Shin et al. group demonstrated that rGO/HAp composites synergistically improved the osteogenic differentiation of the preosteoblasts and confirmed the fact by defining alkaline phosphatase activity and mineralization of calcium and phosphate as early and late stage markers of the osteogenic differentiation [169]. Y.C. Shin et al. also stated that the hydroxyl groups of the HAp microparticles and oxygenated functions (e.g., epoxy, hydroxyl, carboxyl, and carbonyl functions) of the rGO could able to contribute the stronger adhesion or interconnections in Figure 9A,between HAp microparticles and rGO nanosheets.So, it is evidenced that the rGO/HAp composites can preserve their assembly in the culture media and are stable underneath cell culture condition. He also revealed that rGO/HAp composites prompted significant osteogenic differentiation of MC3T3-E1 preosteoblasts with the associated formation of mineralized nodules from von Kossa staining results (Figure 9B).Von Kossa staining was not noticed in the control cultures without any other composites or particles. This observation of Y.C shin, suggest that the late stage marker of osteogenic differentiation was increased by the synergistic effect of rGO/HAp microparticles in absence of osteogenic factors [34,170]. This observation is also consistent with the recent reports i.e gelatinfunctionalized GO could becapably used for the biomimetic mineralization of HAp, leading to support the osteogenic differentiation of MC3T3-E1 preosteoblasts [171]. Furthermore, the rGOincorporated substrata were found to be managing to efficiently increase the osteogenic differentiation by supporting cell-cell interaction or cell-substrata [167,172]. An illustration of the GF-CaP fabrication and its osteogenesis process has been displayed in (Figure 9C) [167]

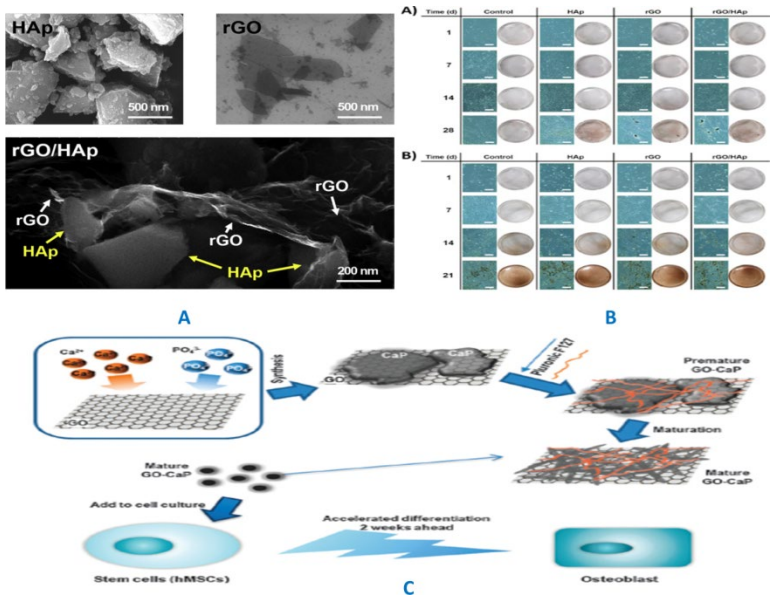

Figure 9. A) Physicochemical characteristics of rGO/HAp composites. (A) FESEM images showed that the HAp microparticles were found to have an irregular granule-like shape with an average particle size of 1080 ± 370 nm and to be partly covered and interconnected by a network of rGO nanosheets which exist as single or few layers. Reproduced with the permission of Elsevier Copyright@2015. Ref. [169] **B)** Image of von Kossa stain in MC3T3-E1 preosteoblasts treated with rGO/HAp composites in (A) BM and (B) OM. Dark brown mineralized nodules were observed only at 28 days in BM, while seen even at 21 days in OM regardless of the addition of particles or composites. All photographs (scale bars = 200 μm) shown in this figure are representative of six independent experiments with similar results.Reproduced with the permission of Elsevier Copyright@2015. Ref. [169]**. C)** Schematic illustration of fabrication procedure for GO–CaP nanocomposites, and subsequent synergistic acceleration of osteogenesis in hMSCs by GO–CaP. Ref. [167].

Chengtie Wu et al. proved that 3D printed β-TCP scaffolds are highly porous materials with a homogeneously large pore structure (nearly 500 μm, (Figure 10a)), and the pore walls cover some micropores of 2μm size(Figure 10a) large pore structure (Figure 10b) for the GO to cover whole pore-wall surface of scaffolds (Figure 10e). Which in turn shows that GO coating β-TCP disks have brilliant

 doi:10.20944/preprints202403.0428.v1

apatite mineralization ability (Figure 10f–h), while pure β-TCP does not keep this facility (Figure 10c) and the GO coating β-TCP contain Ca/P ratio of 1.54 (Figure 10g).Thus it is noteworthy to speculate that the enhanced apatite mineralization of this scaffoldoffersnegative chemical groups too from GO, such as COO^-, for nucleation and crystallization of Ca/P ions in simulated body fluids [173]. Ch.Wu anticipated that the above mentioned features and observations are the main reasons for the nanostructured GO coating β-TCP could improve the proliferation and osteogenic differentiation of osteoblasts [152]. GO coating β-TCP bioceramics suggestively encourages the bone defect repairs with the characteristic cell proliferation, osteogenic gene expression of human bone marrow stromal cells (hBMSCs) by motivating in vitro osteostimulation property. (Figure 11d) indicates hBMSCs on GO-coated β-TCP bioceramics grow healthier with higher cell density rather than on just β-TCP disks within short span.This research group also verified the ionic environment of cell culture media with β-TCP and on GO-coated β-TCP bioceramics and concluded that there was no obvious difference about the released Ca concentrations even though P concentrations are somewhat different in β-TCP and GO-coated β-TCP bioceramics, specifying that modification of GO did not muchaffect the ionic dissolution of β-TCP bioceramics. They havebeen suggested that GO coating itself shows an important role in attracting or increasing the osteogenic differentiation of hBMSCs. Even though there are no research reports on why grapheneoxide has a positive influence on the osteogenic differentiation of stem cells, this research group speculated that the bioactive functions in GO, such as COO and OH, might be one of the key factors to straightaway effect cell differentiation through activating the Wnt-related signaling pathway of stem cells. In agreement with this speculation, the previous reportsexhibited that GO can deliver therapeutic via hydrophobic and electrostatic interactions [9,12,34]. In addition, Chengtie Wu et al. explained that the GO coating on β-TCP ceramics may also adsorb higher number of proteins from the cell culture media, which additionally increases cell response. Many researchers over the world also have raised attention in the mechanism of interaction of GFs with stem cells, which could contribute to increase in vitro osteogenesis.

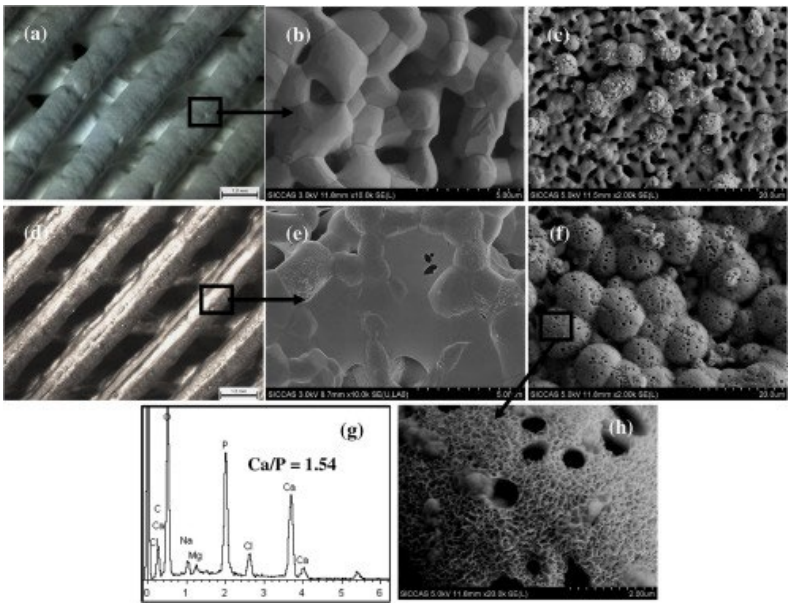

Figure 10. D-printed β-TCP (a) and β-TCP-GRA (d) scaffolds, microstructure of pore walls for β-TCP (b) and β-TCP-GRA (e) scaffolds. After being soaked in simulated body fluids, only a few apatite particles formed on β-TCP scaffolds (c); however, an apatite layer formed on β-TCP-GRA scaffolds (f and h), and EDS suggesting the Ca/P ratio is about 1.54 (g). Reproduced with the permission of Elsevier Copyright@2015. Ref. [152].

 doi:10.20944/preprints202403.0428.v1

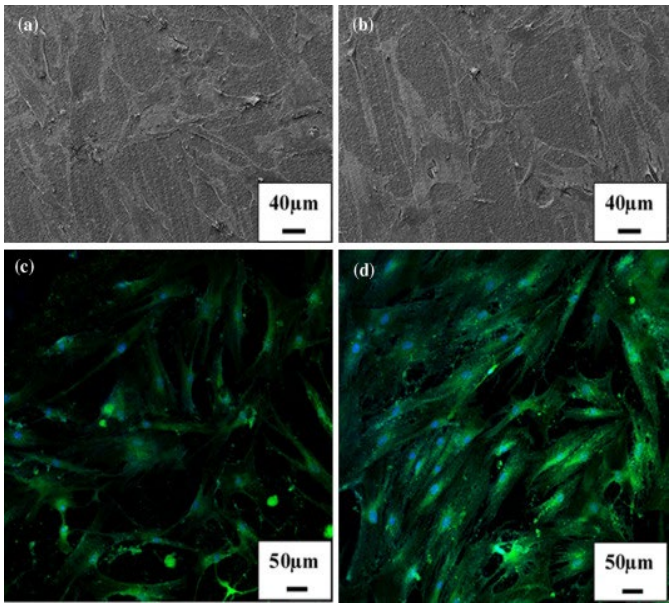

Figure 11. The SEM analysis of cell morphology for hBMSCs on β-TCP (a) and β-TCP-GRA (b) bioceramics after being cultured for 1 day. The confocal fluorescent images for hBMSCs on β-TCP (c) and β-TCP-GRA (d) bioceramics after being cultured for 7 days. Green indicates the structure of cytoskeleton stained by FITC fluorescent dye while blue shows the DAPI-stained cell nuclei. β-TCP-GRA bioceramics could improve cell attachment compared to β-TCP bioceramics. Reproduced with the permission of Elsevier Copyright@2015. Ref. [152].

Jong Ho Lee et al., reported that the rGO/ Hydroxyapatite Nanocomposites could improve the osteogenesis of MC3T3-E1 preosteoblasts and help new bone formation. The combined HAp, rGO synergistically supportedand encourages the natural osteodifferentiation of MC3T3-E1 cells without any hindering of their cell proliferation [10]. The boosted osteogenesis (Figure 12A) was validated from the determination of alkaline phosphatase activity, Alizarin red staining (Figure 12B), Von Kossa staining (Figure 12C) [10], and Immunoblotting effects (Figure 12D) [169]. The surface adsorption of various oxygenatedfunctions presented in the rGO/hydroxyapatite nanocomposites show better cell compatibility and enhanced biofunctionalities for diverse applications.As one of the matrix mineralization markers, the expression of OCN was calculated by an immunoblot analysis (Figure 12D), which was corroborated that the matrix was developed via extracellular calcium deposition as displayed above. Once completed 21 days of incubation, the expression level of OCN in MC3T3-E1 preosteoblasts was tremendously ($p < 0.05$) improved by rGO/HAp composites (Figure 12D$_B$) [169].

 doi:10.20944/preprints202403.0428.v1

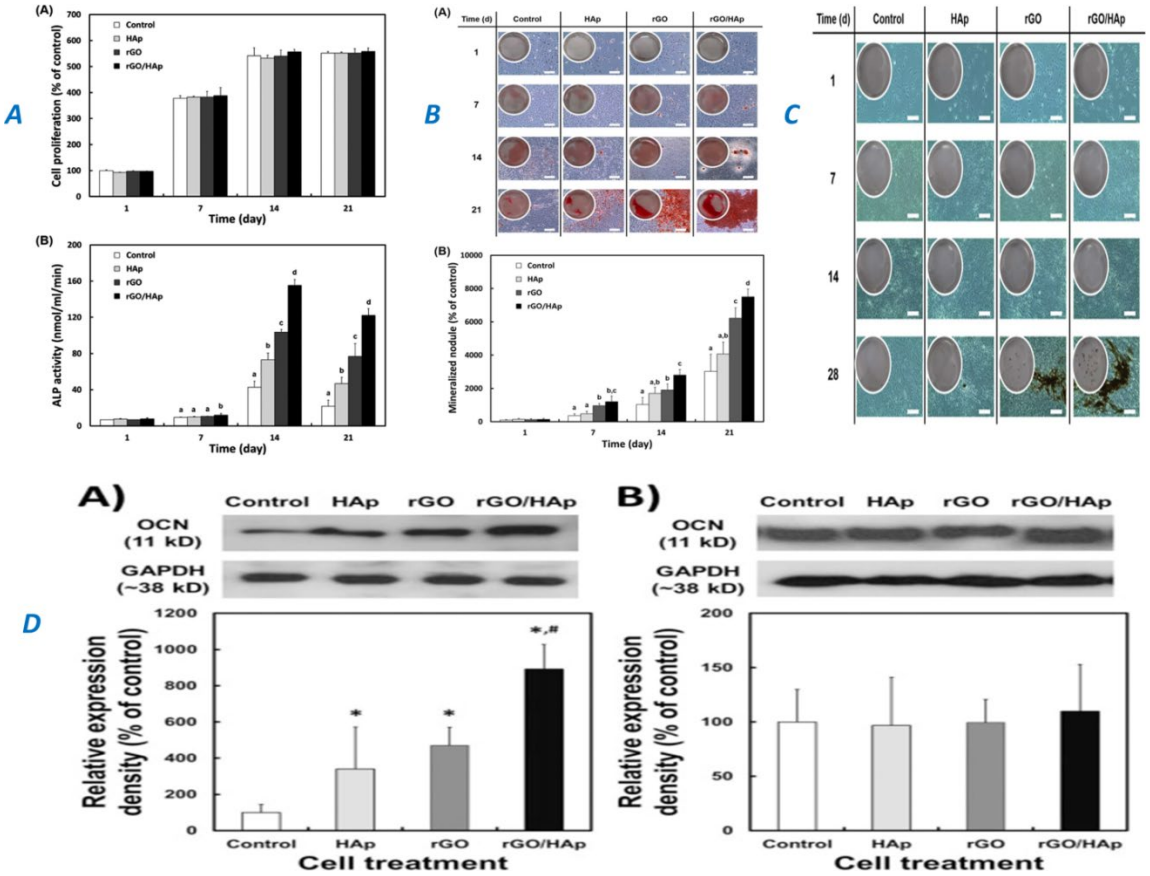

Figure 12. ***A)***Proliferation and ALP activity of MC3T3-E1 cells incubated with a colloidal dispersion of HAp MPs, rGO NSs or rGO/HAp NCs in BM. (A) During the incubation period (up to 21 d), the presence of rGO/HAp NCs resulted in no appreciable decrease in cell proliferation, compared to the non-treated control. (B) Incubation with rGO/HAp NCs for 7 to 21 d significantly ($p < 0.05$) induced ALP activity. The data is expressed as the mean} SD based on at least duplicate observations from three independent experiments. The different letters in (B) denote the significant difference between the non-treated control and the cells incubated with particles or composites, $p < 0.05$. Ref.10, ***B)***The ARS stain and its corresponding extract in MC3T3-E1 cells incubated with a colloidal dispersion of HAp MPs, rGO NSs or rGO/HAp NCs in BM. (A) Increased calcium deposits by rGO/HAp NCswere not related to the cell number (scale bars = 200 μ m). There was a notable formation of calcium deposits byrGO/HAp NCs from 14 d. (B) The dissolved ARS extracted from the staining plates confirmed that the rGO/HAp NCs significantly ($p < 0.05$) increased extracellular calcium deposition in the cells. The data is expressedas the mean ◎} SD based on at least duplicate observations from three independent experiments. The differentletters in (B) denote the significant difference between the non-treated control and cells incubated with particlesor composites, $p < 0.05$. All photographs shown in this figure are representative of six independent experimentswith similar result. Ref.10.***C)***Image of von Kossa stain in MC3T3-E1 cells incubated with a colloidal dispersion of HAp MPs, rGO NSs or rGO/HAp NCs in BM. Dark brown colored nodular staining was observed at 28 d in cellsincubated with rGO/HAp NCs (scale bars = 200 μ m). There was little, if any, crystal formation in cells incubatedwith HAp MPs alone, whereas the cells incubated with rGO NSs alone exhibited strong positivity for von Kossastaining. All photographs shown in this figure are representative of six independent experiments with similarresults. Figures adapted from ref.10. ***D)***Immunoblotting for OCN expression in MC3T3-E1 preosteoblasts treated with rGO/HAp composites in (A) BM and (B) OM. After 21 d of incubation, the expression level of OCN was increased significantly ($p < 0.05$) by rGO/HAp composites. The cells cultured in OM showed no significant difference in the expression level of OCN between the cells treated with and without particles or composites. An asterisk (*) denotes a significant difference between the control and other groups ($p < 0.05$) and number sign (#) denotes a significant difference between the rGO/HAp composite-treated and other groups ($p < 0.05$). The data

 doi:10.20944/preprints202403.0428.v1

is expressed as mean ± SD based on at least duplicate observations from three independent experiments. Reproduced with the permission of Elsevier copyrights@ 2015. Ref. [169].

Rameshwar Tatavartyet al [167] hypothesized that combining GO with an osteoinductive material can synergistically manage the differentiation of human mesenchymal stem cells (hMSCs) headed for osteogenic lineage. Calcium phosphates (CaP) such as HAp are biomimetic composites that are well-recognized to facilitate the bone formation (osteoconductivity) and to ease osteogenic differentiation of hMSCs (osteoinductivity).However, they prepared the GO-CaP to validate this hypothesis for the osteogenesis and proved that the osteogenic differentiation of the hMSCs via immunofluorescence staining of osteoblast markers ALP and osteocalcin as in Figures 13 and 14. It has been mostly hypothesized that the surface features of GF nanomaterials such as surface stiffness, nanotopography and large absorption abilityaffect the molecular paths that regulate the destiny of stem cells [174]. Graphene and grapheneoxide were acting as preconcentrators for chemicals, proteins as well as growth factors on their surface to raise cell differentiation [175]. In GO/CaP, GO surface was generallyshielded by CaP nanoparticles, thereforeunapproachable for direct absorption of molecules. The enriched differentiation may in part have got up from the enhanced interaction between the CaP structure on GO–CaP surface and the intracellular focal adhesion centers of the cells [164]. Moreover, with the incorporation of GO and CaP, GO–CaP biomaterialdemonstratedthe greater stiffness to GO or CaP alone [176]. Such rise in material stiffness could prompt an increasedmechanotransduction effect which has been acknowledged tocontrol stem cell differentiation and thus might payto the synergistic improvement in osteogenesis [177].

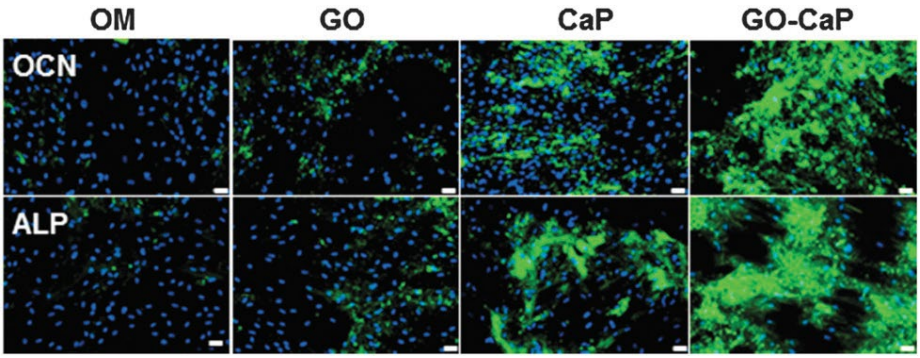

Figure 13. Immunofluorescence staining of hMSC cell culture with FITC labeled (green) osteocalcin (OCN) antibody and DAPI (blue), and Alexa 488 (green) labeled alkaline phosphatase (ALP) antibody and DAPI (blue) after incubation with control osteogenic medium, GO, CaP, and GO–CaP for two weeks. Scale bars represent 20 mm. Ref. [167].

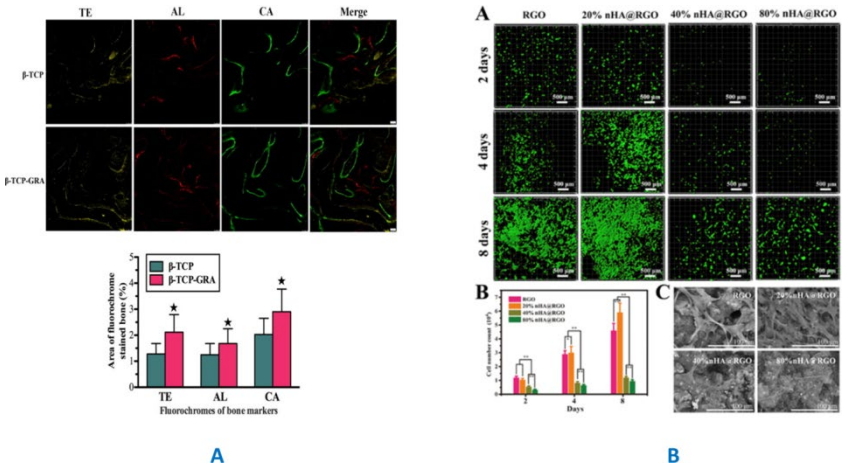

Figure 14. A) Sequential fluorescent labeling; yellow, red, and green color represent labeling by tetracycline (TE), alizarin red (AL), and calcein (CL) for in vivo bone-forming ability of β-TCP and β-

 doi:10.20944/preprints202403.0428.v1

TCP-GRA scaffolds after being implanted in the cranial bone defects of rabbits for 4 and 8 weeks (c), respectively. The scale bar is 50 μm. ⋆Significant difference between the β-TCP and β-TCP-GRA groups ($p < 0.05$). Reproduced with the permission of Elsevier Copyright@2015. Ref. [152]., B) The rBMSCs proliferated on the scaffolds detected by live cell staining (A) and cell count (B) for 2, 4, 8 days. The SEM image (C) exhibit the rBMSCs growth on the scaffolds for 8 days after seeding. The 3D fluorescence photos were captured using z stack image collection with 40× magnification. Reproduced with the permission of Elsevier copyright@2017. Ref. [148].

As reported earlier [178], GFs and their derivates consent the attachment of stem cells and stimulate their development and their differentiation to the osteogenic lineage.GO surfaces could be possibly used as delivery transporters for proteins. This probability is supported by the specifics of GO sheets which holds hydrophobic π domains in the core area and ionized functions around the edges of GO. These characteristics significantly increase its interactions with proteins with hydrophobic and electrostatic interactions even in GF-CaP [9]. Previous studies have stated that osteoblasts adhered well and proliferated on the surface of rGO- or GF-HAp hybrid nanomaterials, which proposes that these composites induce 3D adhesion of osteoblast cells and continue cell viability by giving microenvironment alike to that found in vivo [179–181]. ζ potential of rGO-coated BCP composite having stable surface and surface charge of -14.43 mV, which specified rGO-coated BCP bone graft material was designed by electrostatic interactions between BCP and rGO. [9] and this feature of GO-BCP helps on cell growth. The cell growth is also mainly dependent on its structure, size, and concentration.Jeong-Woo Kim et al. demonstrated that the cell viability was decreased at rGO concentrations >100 μg/mL, but was sustained above 80% at concentrations <62.5 μg/mL. Thus he suggested from his results, rGO has no harmful properties and it is a non-cytotoxic at concentrations <62.5 μg/mL [9].

On the other hand, J.H.Lee demonstrated that the osteogenic differentiation of hMSCs was improved by rGO-coated HAp nanomaterials when incubated in basal media in absence of osteoinductive agents. Moreover, he also stated that the osteogenic action mediated by rGO-coated HAp nanocomposites was further increasedwhile cells were cultured in osteogenic medium. An initial coverage of cells to a colloidal dispersion of rGO-HAp material and consequently increased contact with these composites, which in turn enabled intracellular signalling, may proposed as a feasible explanation. However, his results are not clearly proved the mechanism, involved in intracellular signalling pathways. However, his studies supported the rGO-coated HAp composites could be potent factors in helping the spontaneous osteogenic differentiation of osteoprogenitor cells. Thus these rGO-HAp materials might be potential candidates for scaffolds in bone tissue engineering, stimulators for stem cell differentiation and constituents of implantable expedients, due to their biocompatible and bioactive assets [34].

4. GF-CaP Based 2D & 3D Layered Nano Composites and Influences

Earlier studies specified that 2D GFs can be coated on solid substances of substrates through several physical and chemical methods, and the resulted GF nanomaterial coatings may significantly increase the interfacial properties, such as the mechanical, electrochemical, anticorrosion and biocompatibility so, providing them good application potential for the surface adjustments of biomedical implants [182]. Recent developments have exposed that GF-based 2D and 3D substrates promote the adhesion and proliferation different cell lines such as human osteoblasts and stem cells [183]. Human osteoblasts can adhere well to the GF coated materials with a confluent monolayer of normal fibroblast-like morphology, while they exhibit separate round-shaped cells on grafts [184–187]. From the previous reports. [34], it is revealed that, once seeding cells (hMSCs), the cell suspension is incubated with a colloidal dispersion of HAp,rGO nano particles or rGO-coated HAp composite materials in basal media till they were grown as monolayer cultures. Jong Ho Lee et al. [34] demonstrated as, it was more advantageous forthe cells which were primarily exposed to rGO-coatedHAp material in 3D culture instead of 2Dplated monolayers and thus the effectiveness of cell contact withthese coating composites was improved, which in turn simplifiedintracellular signalling

 doi:10.20944/preprints202403.0428.v1

and succeeding osteogenic activityin hMSCs.Moreover, he also determined the better ALP activity of hMSCs incubated with rGO-coated HAp material in 3D culture was more potential to that in the 2D incubation system since the composite in basal media was treated with as-grown monolayers of cells. Furthermore, the intensity of alizarin red staining was highly increased the 3D incubation system as shown in Figure 15. The same trend was also observed in an immunocytochemical analysis for osteogenic markers, after 14 days of incubation in basal media in absence of osteogenic factors, rGO-coated HAp composites substantially upregulated the expression of OPNand stimulated de novo expression of OCN in hMSCs as seen in Figure 15. Conversely, non-treated cells exhibited few, if any, expression of both the osteogenic markers. This implies that rGO-coated HAp materials could promote the impulsive osteogenic differentiation of hMSCs in a 3D environment. This is consistent with the reports i.e graphene-cell biocomposites increases pellet generation and differentiation of human bone marrow-derived hMSCs headed for the chondrogenic lineage in preconcentrating growth factors [186–188].The coated graphene oxide also enhanced the calcium deposition in hMSCs.It is suggested that the graphene layer tolerates a noncovalent bridging of protein nutrition and osteogenic growth factors on its flat surface through electrostatic interactions, π-π stacking or hydrogen bonding, thus helping the adhesion and differentiation of hMSCs.Besides, it has been found that the oxygen contents on its surface of rGO-HAp affect the osteogenic differentiation due to the altered interaction between rGO-coated HAp materials and growth factors or proteins [185–189].

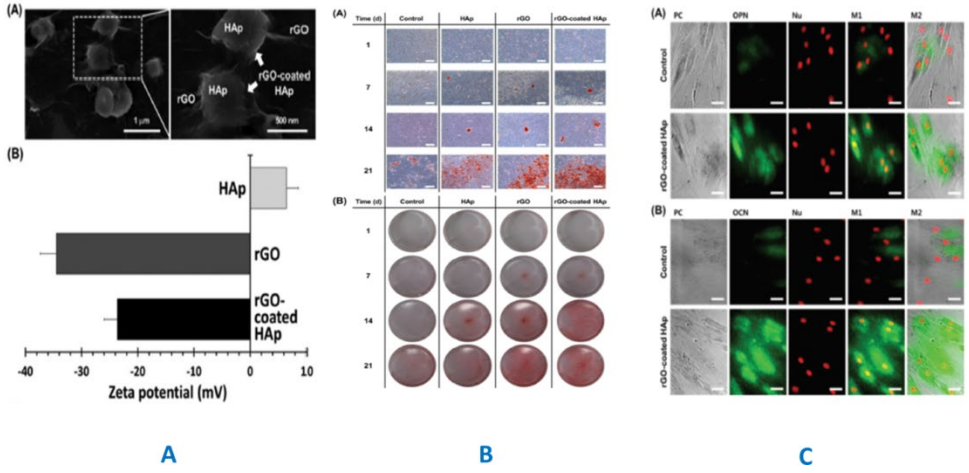

Figure 15. A) Physicochemical characteristics of rGO-coated HAp composites. (A) FESEM images of rGO-coated HAp composites showing rGO sheets surrounding HAp microparticles and covering the HAp MP surface. (B) Surface charges of HAp microparticles, rGO NPs and rGO-coated HAp composites indicating the formation of rGO-coated HAp composites via electrostatic interactions between HAp microparticles and rGO NPs. Reproduced with the permission of royal society of chemistry@2015. Ref. [34] **B)** ARS stain and its corresponding extract in hMSCs incubated with a colloidal dispersion of HAp microparticles, rGO NPs or rGO-coated HAp composites in BM. (A) Increased calcium deposits by rGO-coated HAp composites were not related to the cell number (scale bars = 200 μm). (B) There was a notable formation of calcium deposits by rGO coated HAp composites from 14 to 21 days indicating that HAp microparticles and rGO NPs synergistically induce calcium deposition in hMSCs. Reproduced with the permission of royal society of chemistry@2015. Ref. [34]**. C)** Immunostaining for osteogenic markers for hMSCs incubated with a colloidal dispersion of rGO-coated HAp composites in BM for 14 days. Culture of hMSCs with a colloidal dispersion of rGO-coated HAp composites stimulated de novo expression of the osteogenic markers OPN (A) and OCN (B) (scale bars = 20 μm). These data confirm that rGOcoated HAp composites promote the spontaneous osteogenic differentiation of hMSCs. All photographs shown in this figure are representative of six independent experiments with similar results (PC: phase contrast, Nu: nucleus, M1: merge of OPN (or OCN) and Nu, M2: merge of PC and M1). Reproduced with the permission of royal society of chemistry@2015. Ref. [34]**.**

 doi:10.20944/preprints202403.0428.v1

On the other hand, the pure graphene multilayer dropped by the CVD technique can offer a favorable biocompatible 2D interface for proliferation, adhesion, and differentiation of hMSCs and neural stem cells (NSCs).Diverse from pure graphene, GF-CaP may display specific interactions with stem cells for the cell morphology due to the rich oxygen functioned flat surface (2D) of the GF materials [9,34,183]. Loh et al. find that the modified GO materials can be directly cross-linked at the air-water interface via the dip-coating technique, whereby the coated film shapes as highly wrinkled films.In the interim, the highly wrinkled grapheneoxide film can prompt osteogenic differentiation without any chemical inducers; it is thought that the greatly wrinkled structure shows a driving force en route for an osteogenic differentiation [180–187]. The nanoscale geographical scaffold surfaces can also present anexceptional extracellular microenvironment that impacts the activities of a cell or stem cell, such as a cell shape, growth, adhesionand differentiation [181–188]. The facilely established large-scale, crumpled graphene or GO layers-based structures are also found to be gifted for guiding cell aligned growth. Since the hierarchical and high-aspect-ratio shaped constructions are fabricated by using the wrinkling and localized ridge uncertainties of GF coating films on prestrained elastomer substarte contents, mechanicallystretching the elastomer substrate can effortlesslymanage the patternstructures, thereby facilitating the optical transmittance, wettability, cell alignment and cell adhesion on the substrates. Thus, utilization of electrospinning process to produce nanofibrousmatrix as micropatterned substrates and could be the other facile and inexpensivemethod for the construction of GF-coated decorative scaffolds.

Besides, for GO-coated materials, water molecules can freely penetrate into GO interlayers while filtration due to the hydrophilic character of the GO sheets, which can later, applied for the water separation from the organic solution. Further cross-linking of GF layers may greatly increase the mechanical characteristics of GO-coated films, in terms of covalent cross-linking or divalent cations (Ca^{2+}) to bridging with the hydroxyl and carboxylic acid groups [34,187].

Synthetic 3D architectures of GF-CaP family can generate microenvironments alike to ECM, which thus increases cell adhesion, growth, and differentiation due to thephysiological significance of the ECM structure.The design of bioactive scaffolds is an important goal for tissue regeneration.GFs, such as graphene, GO, rGO, and organically/inorganically modified graphene, have been demonstrated to increase the adhesion and growth of mammalian cells including osteoblasts, fibroblasts, stem cells and microbial cells. So, it is significant to explore how the GF-CaP-based 3D scaffolds affect the adhesion and growth of cells. Recently, 3D scaffolds consisting of GF-CaP have been successfully produced by different procedures [9,34,147,173].

The GO coating was synthesized on the surface of 2D disc circles and 3D scaffolds of β-TCP ceramics by soaking ceramic scaffolds in GO-H_2O suspension in combination with following heat treatment. As displayed in Figure 16a, surfaces of β-TCP disks are flat and smooth. Nevertheless, later, being coated with grapheneoxide, the surfaces turned rough with diverse GO nanosheets (Figure 16b,d). The β-TCPs are white, and afterward modification with grapheneoxide, the whole β-TCP disks are gray (Figure 16c), representating that GO can covers the total surface of β-TCP disks. The characteristic C1s peaks of XPS agreeing with C-C, C=O and carboxyl (COOH) and are distinct for GO/β-TCP (Figure 16e,f) which thus subsidize to the better hydrophilicity on the disk surface (Figure 16h). Once the GO modification, there was no phase has been changed for β-TCP bioceramics (Figure 16g). As displayed in Figure 14, GO-Coated-β-TCP disks enhance the hBMSCs grow better with higher cell concentration than those on β-TCP disks [152].

 doi:10.20944/preprints202403.0428.v1

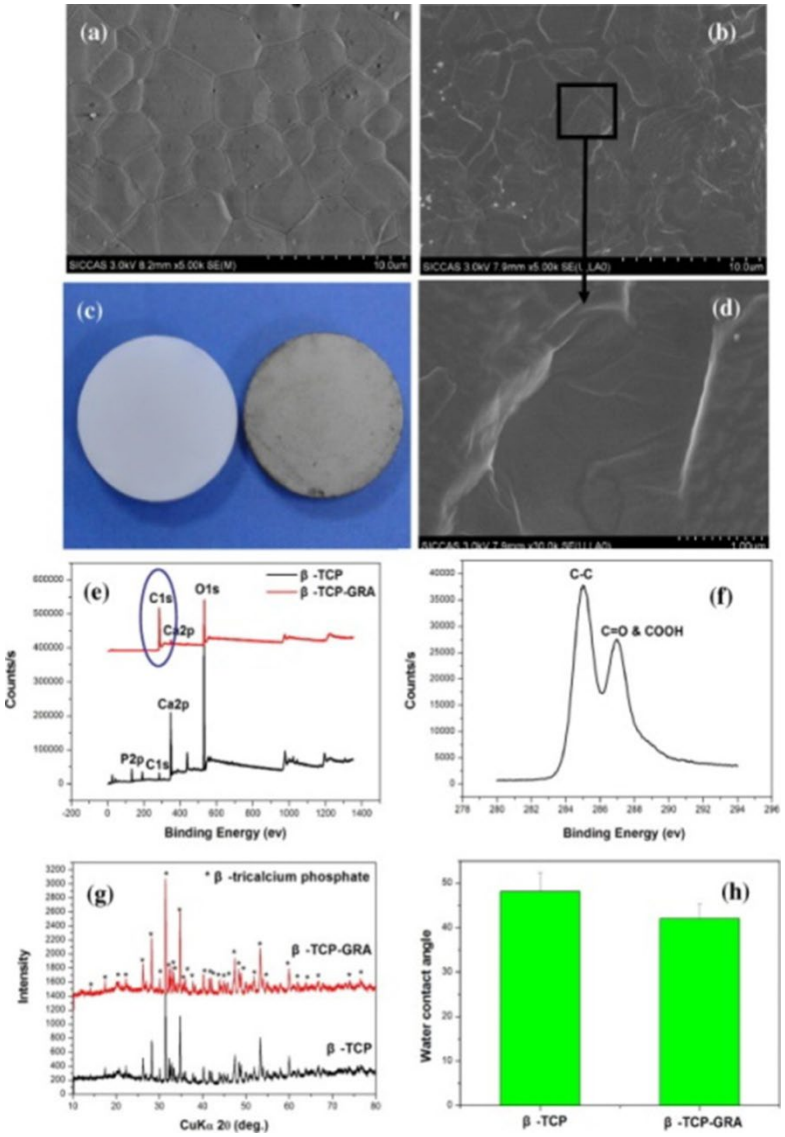

Figure 16. a) SEM for the prepared β-TCP (a) and β-TCP-GRA (b and d) bioceramic disks, (c) the whole morphology of β-TCP (left) and β-TCP-GRA (right) disks, (d) the higher magnification image. Arrows point to graphene oxide. (e) XPS analysis, (f) the C1s peaks for β-TCP-GRA bioceramics, (g) XRD analysis, and (h) the water contact angle (degree) for the prepared β-TCP and β-TCP-GRA bioceramic disks. Reproduced with the permission of Elsevier Copyright@2015. Ref. [152].

However, the cellular mechanisms involved in the process of GF and GF-CaP materials applications in osteogenic differentiation of stem cells is remain unclear. Few reports said that the 3D graphene foam and 2D graphene substrate can explore key features on both the genomic and protein stages that are involved in the osteogenic differentiation [34,190,191]. It has been found that 2D and 3D graphene scaffolds induce differentiation of stem cells into mature osteoblasts at higher levels than the glass or PS substrates. Bone-related genes and proteins were upregulated on graphene regardless of the use of the osteogenic medium. The high gene expressions of MHY10 and MHY10-V2 on 2D and 3D graphene scaffolds recommend that their physical characteristics may have a significant part in the improved differentiation. In conclusion, it is suggested that both chemical and physical properties of GF-CaP act synergistically while presiding osteoblastic differentiation of stem cells.

5. Emerging Biomedical Applications of GF-CaP Based Architectures

Previous reports revealed that biphasic calcium phosphate was coated at varied levels with GF BCP and connected by GF network [9,12,34,152]. Also, the previous studies have stated that

 doi:10.20944/preprints202403.0428.v1

osteoblasts adhered well too and proliferated on graphene-hydroxyapatite hybrid nanomaterials, which advises that these nanomaterials induce the 3D (three dimensional) adhesion of osteoblast cells and sustain cell viability by availing a microenvironment alike to that compared to in vivo [34,152]. Reports revealed that the ID/IG ratio of reduced graphene oxide (1) is little lesser than GF-CaP (1.05) which reveals the increased surface area of the desired nanomaterial. Some studies proved, the cytotoxicity of reduced graphene oxide involves the generation of oxidative stress response [9] too. The previous results [9] suggest GFs have no harmful effects and is non-cytotoxic at concentrations < 62.5 μg/mL. Recent reports also revealing that, after 8 weeks of surgery, entire volumes of new bone (mm 3) were determined by micro-CT, and exhibited that the GF-coated BCP groups showed meaningfully more new bone formation than the selected control group. The GF group and BCP mixture showed the significant total volume of new bone. Some Micro-CT and histometric analysis displayed that the GF group exhibited the highest new bone area. Results also suggesting as the percentage of GF is improved, bone regeneration capability is also enhanced, but when the GF percentage exceeds a definite threshold level, GF cytotoxicity reduces osteoblast viability. The physicochemical characteristics of graphene are likely responsible for its improvement of osteogenic differentiation. The wrinkles and ripples existing on GFs surfaces may affect osteogenic differentiation, [9,34,40,65,152] as these structures support cell wharf and an increased cytoskeletal tension. [143–151] Furthermore, GFs can adsorb biomolecules (dexamethasone) and proteins (β-glycerophosphate) and these could help cell differentiation [12,34]. Thus, GF-coated BCP bone graft material accelerated fresh bone formation. In addition, adhesion and bioactivity of multilayer GFs have been exploited to improve the detection resolution of several wet whole cells via TEM in an intact culture environment [192]. J.W.Kim et al. [9] have also fabricated graphene oxide-coated biphasic calcium phosphatecell aligners with matching mechanical properties for the bone defect repairs. The designed material is multifunctional and soft cell-culture platform which is able to bring into line the incubated cells and in situ monitoring the physiological behaviors of stem cells during their growth and differentiation.Beyond the in vitro cell imaging, GF-CaP electrodes show abundant potential for in situ cell and tissue engineering.Integrated advantages of biology, electrical, and mechanical stuff are always desirable for materials used in cell and tissue monitoring [193].

Metal and silicon have been extensively used in fabricating reasonable and conventional prosthetic maneuvers. Nevertheless, their poor chemical-resistance in physiological locations, relatively significant electrical noise, rigid mechanical properties, and high inflammation potential result in abundant limitations in biomedical engineering applications. [194–196] Recent developments in designing GF-CaP [152,155,165] are focusing on making them as flexible, and bioactive and nanostructured materials as to improve the tissue compatibility and integration.Therefore, GF-CaP based nanomaterials present hopefulforthcoming in succeedingconductive tissue-interfaces, particularly the conductive graphene [197]. Because of the outstanding and exceptional properties, like mechanical stability, electrical conductivity, thermal conductivity, bigger specific surface area, very easier chemical modifications and finally good biocompatibility, it has been believed that GF based flexible could be applied for tissue monitoring claims.

Recent studies have showed that, when GFs are applied for surface coating of implants or membranes, no clear blood and cell toxicity has been detected [198–200]. It is assumed that the reduced “face-to-edge” interaction between the cell membrane and GFs-based coatings would be the key object for their increased cell adhesion and proliferation ofmodified grafts. Beyond all these mentioned emergencies,spray-coating is one of the best ways to attain a homogeneous and dense surface coating, and Li research group have described the preparation of the HA-graphene based nanocomposite thin film coatings by liquid precipitation method and the assistance of vacuum cold spraying [180]. The acquired HA-graphene complex coatings retention intact nanostructured morphology and increased spreading and proliferation of osteoblast cells. The electrodeposition of GFs onto conductive substrates is another kind of popular surface coating method.Rhee et al. suggested and reported to coat silver/HA/graphene (Figure 17) porous films on titanium surfaces using electrophoretic deposition [181]. It is also demonstrated that the silver/HA/graphene coated

 doi:10.20944/preprints202403.0428.v1

substrates display a diminished amount of surface cracks and increased thermal stability and mechanical property on compared to the graphene-free coatings.The bioactivity examinations revealed that the coated substrate owns better resistance to the body fluid stimulated corrosion and improved antibacterial activity against *E. coil* and *S. aureus*; whereas, no obvious cytotoxicity has been noticed for peripheral blood mononuclear cells.

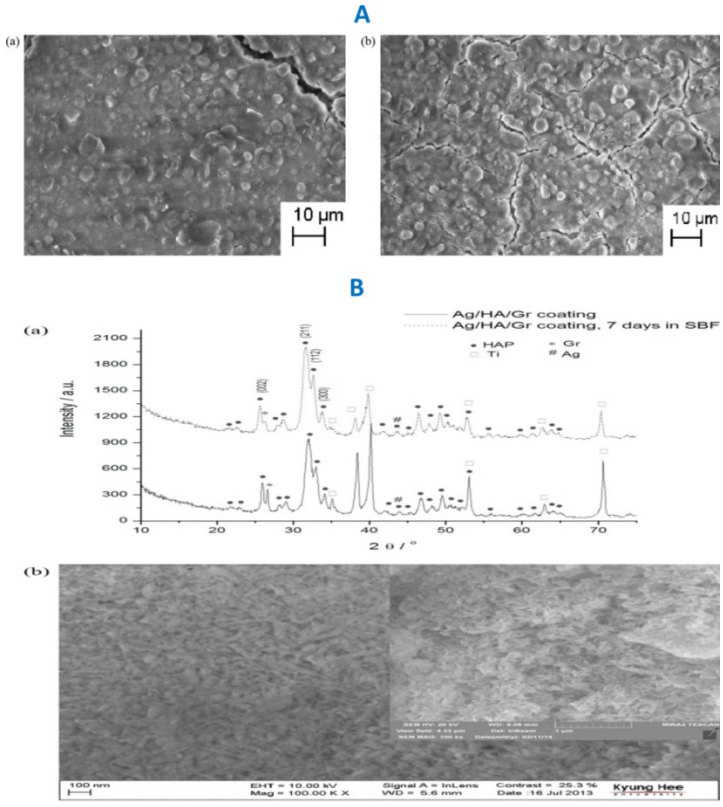

Figure 17. A) FE-SEM micrographs of the Ag/HAP/Gr (a) and Ag/HAP (b) coatings, magnification 1000× **B)** XRD patterns (a) and FE-SEM microphotographs (b) of the Ag/HAP/Gr coating before and after immersion in SBF (inset: Ag/HAP/Gr coating, 7 days in SBF, 37 °C). Reproduced with the permission of Elsevier Copyright@2015. Ref. [120].

In the same way, highly biocompatible composite coatings of HA-GO [140], HA-gelatin-GO [201] and HA-chitosan-GO [9,10,139,173,202] designatedassemblies on titanium have also been accomplished. These materials display good biocompatibility for the period of incubation with MG63 cells (Figure 18c).Once an incorporation of GO, the coated films turned out to bea porous, additional corrosion resistant, and extremely cell compatible.

 doi:10.20944/preprints202403.0428.v1

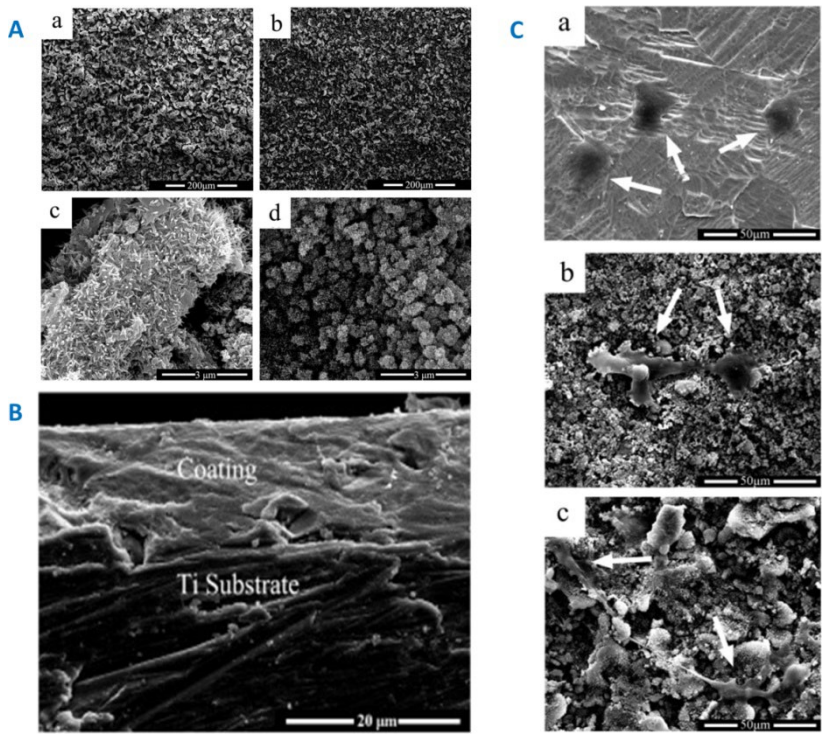

Figure 18. A) Surface morphologies of the pure HA coating (a) and 100 μg/mL GO/HA composite coatings (b) in low magnification SEM images; Surface morphologies of the pure HA coating (c) and 100 μg/mL GO/HA composite coatings (d) in high magnification SEM images**. B)** Cross-section of the 100 μg/mL GO/HA composite coating.C) SEM micrographs of MG63 cells cultured on pure Ti (a), pure HA coating (b) and 200 μg/mL GO/HA (c) composite coatings for 24 h. The white arrow heads point to the cells. Reproduced with the permission of Elsevier Copyright@2016. Ref. [140].

Even some other calcium based HAp has been broadly used as coating resources for metal implants to increase biocompatibility and accelerate early cellular relocation.Conversely, the deprived fracture toughness and wear resistance limited their long-standing usage once the implantation. J.W.Kim et al. alternatively directed that the GF-supported calcium phosphates could be used to reinforce the mechanical properties of any kind of calcium based bioceramic coatings [9]. It was also observed that the GO coating on calcium phosphates can induce rapid production of HAp layer(Figure 19), thus generating better adhesion and growth of stem cells.

 doi:10.20944/preprints202403.0428.v1

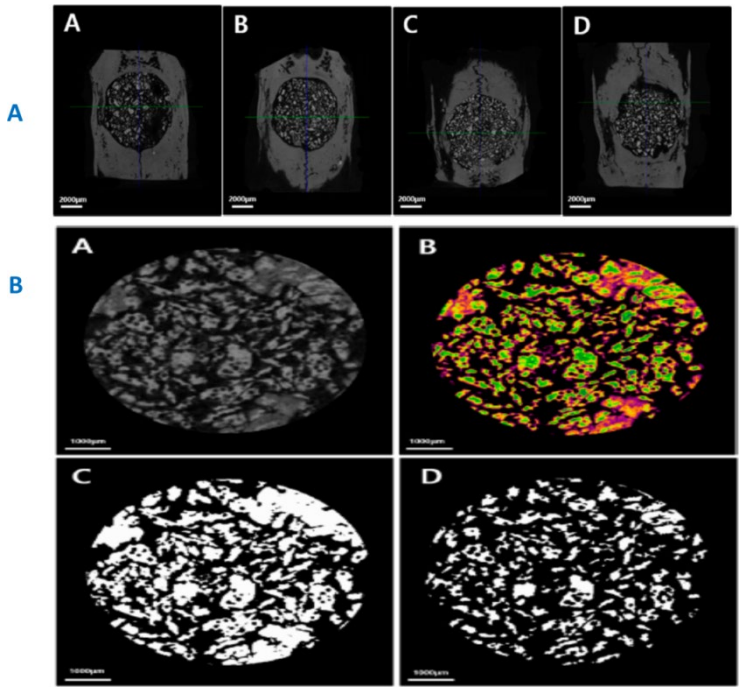

Figure 19. A) Micro computed tomographic images. A) Control group ; B) rGO2 group ; C) rGO4 group; Ref. [9]. D) rGO10 group **B)** Micro-computed tomographic (CT) images of regions of interest. (A) Reconstructed image; (B) Color image (yellow and green-bone graft material and orange and purple-new bone); (C) Total bone (bone graft material and new bone) image; (D) Bone graft material image. Ref. [9].

The GF-CaP biomaterials have been proven to function as effectual coating composite materials compared to pure HA coatings alone. The addition of GF materials into calcium phosphate coatings can minimize the potential of surface cracks with enhanced adhesion strength and resistance to body fluid induced corrosion. Furthermore, the GF-CaP coating revealsmuch higher viability and cell adhesion compared to the HA uncoated and coated nano metal substrates. The above literature reportssuggest that coating GF nanomaterials on substrates or implants can expressivelyincrease the interfacial assets of biomaterials and thus increase their performance in bone tissue engineering applications [9,12,139,152].

There are few more evidences on GF-CaP mechanical properties by Y. Zhao et al. [157]. HRTEM revealed that the detailed information about microstructures. From Figure 20a, it can be seen that graphene nano platelets (GNPs) are located on the grain borders bending and succeeding the shape of grain, where the grain size is about 0.5–1 μm, which is consistent with the observation in FESEM images [157]. A single graphene nano particle with thickness of 5 nm was displayed in Figure 20b, which could be distinguished easily via its characteristic lattice. Graphene nano particles are exceptionally thin, while easy to agglomerate. Overlay GNPs with thickness of about 20 nm are situated between two grains (Figure 20c), and the lattices of GNPs and grains could see clearly. Also, the tight bonding between matrix and GNPs was clearly displayed in Figure 20d, and no noticeable diffusion layer is perceived at the interface. The tight bonding is helpful to transferring load between GFs and the matrix and to establishingthe bridging, eventually leading to the enhanced mechanical properties.

 doi:10.20944/preprints202403.0428.v1

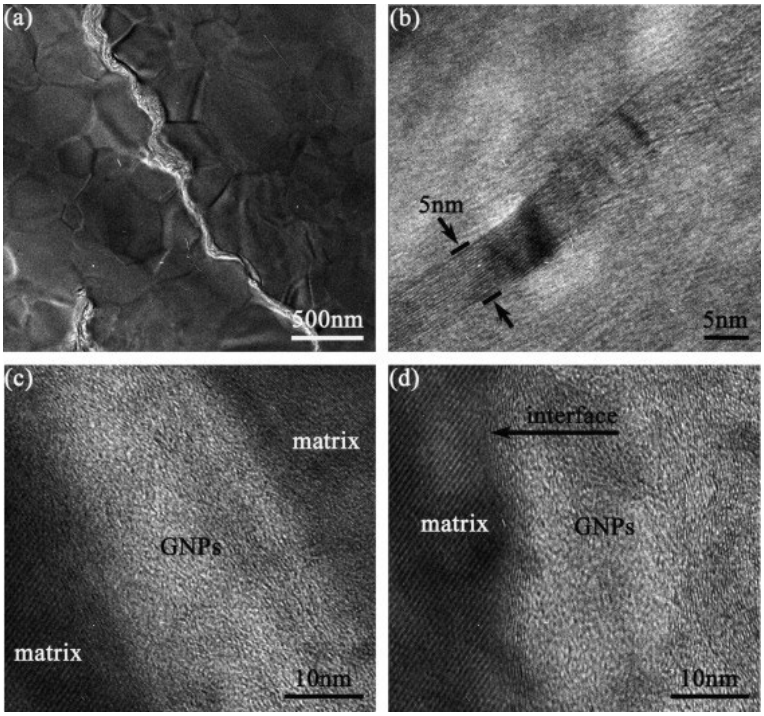

Figure 20. HRTEM images of 1.5 wt% GNPs/BCP composite: (a) GNPs locate at grain boundary, (b) a single GNP with thickness of 5 nm, (c) overlapped GNPs locate between two grains, and (d) the interface of GNPs and matrix. Reproduced with the permission of Elsevier Copyright@2013. Ref. [157].

Recently, Weibo Xie et al. [203] reported, the mechanically robust 3D graphene–hydroxyapatite hybrid bioscaffolds (GHB).As shown in Figure 21a–c, the surface of the GF scaffold was mineralized with electrodepositing circumstances of -1.4 V and 30 ^{0}C for 30 min. The related SEM images at dissimilar scale bars (200, 50, and 5 μm, respectively) display that the hydroxyapatite or calcium phosphate composite is conformably covered on the surface of micro-branches within the graphene foam substrate. Though the pore size of graphene foam is somewhat reduced, there is no hole-blocking phenomenon that occurred. The high magnification image demonstrates the lamellar-featured structure of the calcium phosphate composite on multiscale with the usual thickness of 3.6 ±0.5 μm. Furthermore, the effect of electrodepositing conditions on the morphologies of calcium phosphate composite was further examined at dissimilar temperature of 60 ^{0}C (-1.4 V/60^{0} C for 30 min), as demonstrated in Figure 2d–f. Fascinatingly, besides the same uniform and laminar deposition of CP composite, there are importantchanges of the morphologies with more regular and smaller grain size displayed, leading to additional enhancements of density and toughness for the mineralized graphene foams. As shown in Figure 21B(a–c), the TEM images displayed that calcium phosphates possess flake micrographs with laminar like crystal structures by various sizes, which is consistent with the results obtained by SEM characterizations as presented in Figure 21A. These materials were then further checked in their bone related applications which can show an improved osteoconductive and biocompatible performance. This group also proved the high elasticity of the composite with recoverable compressive strain up to 80% (Figure 22a), and significantly improved strength with Young's modulus up to 0.933 MPa compared with that of pure GF template (~7.5 kPa) [Ref from original Reference]. As shown in Figure 22b, the original dry and stiff graphene–hydroxyapatite hybrid bioscaffold sample was wetted in culture solvent, and thenshifted away with the structure keeping tough and robust. Such superior act of GHBs resisting large deformation and tension-force-induced shrinkage increases them to be used broadly as biocompatible scaffolds.

Preprints.org (www.preprints.org) | NOT PEER-REVIEWED | Posted: 7 March 2024 doi:10.20944/preprints202403.0428.v1

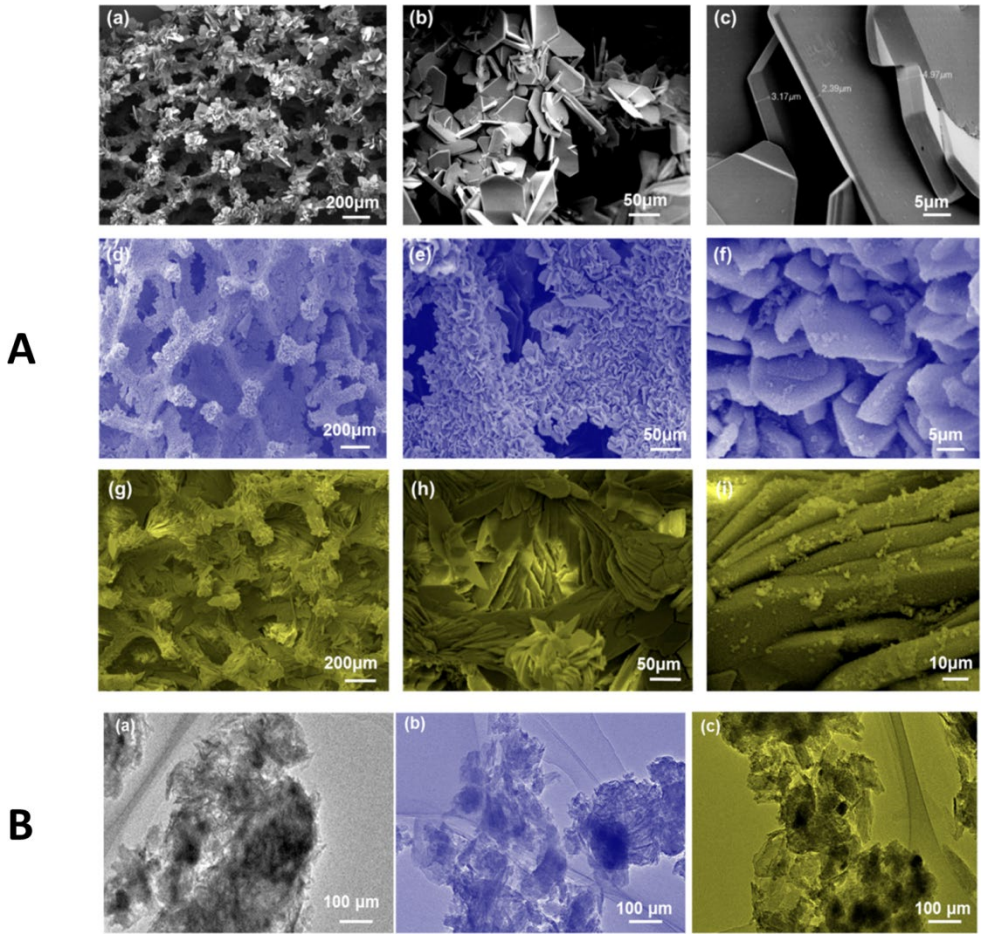

Figure 21. A)SEM images of graphene–hydroxyapatite hybrid bioscaffolds (GHBs) for different electrodeposition conditions. (a–c) 30 ^{0}C and -1.4 V for 30 min. (d–f) 60 ^{0}C and -1.4 V for 30 min. (g–i) 30 ^{0}C and -2.1 V for 30 min.B) TEM micrographs of GHBs with similar deposition conditions. (a) 30 °C and −1.4 V for 30 min b) 60 ^{0}C and -1.4 V for 30 min. (c) 30 ^{0}C and -2.1 V for 30 min.Adapted from ref. [203].

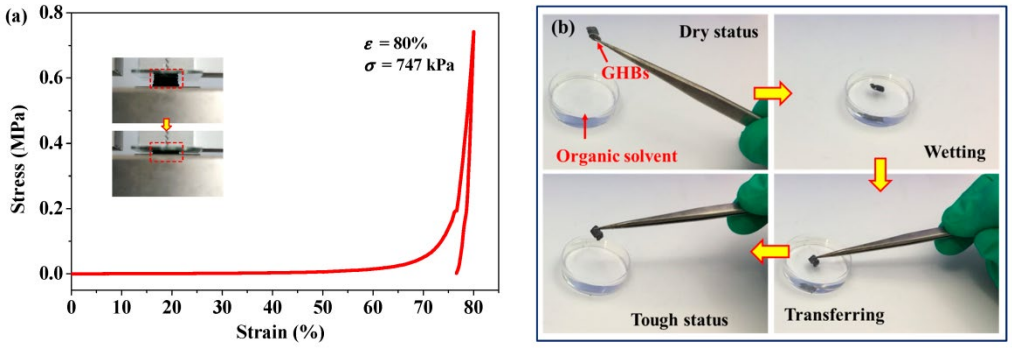

Figure 22. The comparative mechanical compression test of GHB samples with maximum strain up to 80%. Inset is the snapshots during compression. (b) The validation of mechanical robustness of GHB sample during operation in solvent conditions. Adapted from ref [203].

The health status and cytostatic activities of MC3T3-E1 cells were also evaluated by acridine – orange-ethidium bromide (AOEB) double staining assay. Studies have exposed that AO reagents can only enter into the living cells with the fluorescence appearing as green color, whereas EB only enters into dead cells to be orange-red [204]. Figure 23 displays the AO–EB staining fluorescence images of MC3T3-E1 cells co-cultured on 2nd day and 4th day, where cells in the all images are almost green.

 doi:10.20944/preprints202403.0428.v1

The total cells within both 3D graphene foams and GHBs rise with the prolongation of culture time (2–4 d). Relatively, the 3D GHBs determine the higher densities of cells on the surface than that of the GF all over the whole incubation period, which is consistent with the MTT results [203]. Such prior actauthenticates that both kinds of scaffolds do not have cytotoxicity and can offer compatible substrate for cell adhesions. So, it is essential to show that 3D GHBs are more capable of endorsing the proliferation of MC3T3-E1 cells.

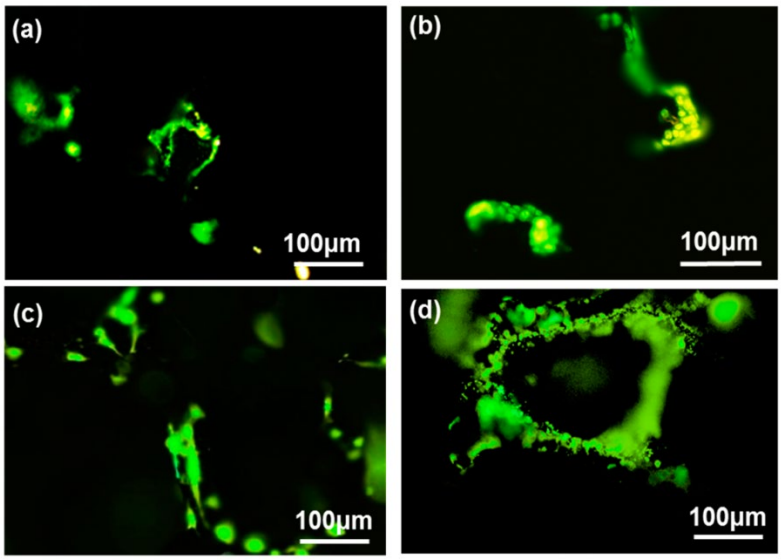

Figure 23. Flourescence microscope images of the MC3T3-E1 cells after acridine orange-ethidium bromide (AO–EB) double staining. (a) and (b) 2nd and 4th days on 3D GF, respectively. (c) and (d) 2nd and 4th days on 3D GHBs, respectively. Adapted from ref. [203].

Conversely, the GF-CaPs materials possess some disadvantages such as using expensive experimental set ups eg. Autoclaves. Inability to observe the crytal as it grows in synthetic process.In situ setting with particle leaching has numerous drawbacks: a) because the porogens inside the materials have limited acquaintance to body fluids, the solubility of the particles or degradation may be compromised, which might lead to limited porosity. b) The in vivo dissolution of some particles may affect the hyperosmosis. c) Some porogens may raise the paste viscosity and obstruct the injectability of GO-CaP. Therefore, pre-fabricated calcium phosphate scaffolds have been established to allow more gentle control of the setting procedure and macroporous GO-CaP construction of the scaffolds before in vivo implantation.Hence, to resolve the drawbacks, recently, three-dimensional (3D) printing has rapidly advanced to allow the fabrication of bone regeneration scaffolds. 3D printing is a preservative manufacturing procedure in which geometrical data are used to generate 3D structures by placing materials layer by layer. 3Dprinted graphene based CPC scaffolds are preferred over customization to meet the precise needs of each defect.The benefits for clinical applications include tranquil adaptation and fixation, minimized surgical time, satisfactory esthetic results and minimal waste products.So, new tissue engineering methods utilizing CPC scaffolds with co-culture and tri-culture represent exciting alternative strategies that warrant further research for continued improvement to achieve wide clinical applications.

6. Standpoint and Future Directions

GF-CaP have been engaging more and more attention as an evolving stand in the fields of material science, chemistry, biomedical engineering due to their superior mechanical properties, higher surface area, outstanding thermal and electronic properties, as well as easy chemical modifications. Rather than their uses in nanomedicine for phototherapy and drug/gene delivery GF-CaP have shown tremendous interaction and adhesive possessions for protein, microbial and mammalian cells, which make GF-CaP hybrid designs potential stages for multifunctional biological

 doi:10.20944/preprints202403.0428.v1

applications.In this review, we have concise the recent developments in the construction of GF-CaP architectures for biological applications in cellular signal detection, stem cell engineering, implant coating, bone tissue regeneration. It is believed that the design of GF-CaPs hybrid architectures have an auspicious future and will draw benefits across a broad range of research fields.

Inspite of the great efforts that have been taken to construct GF-CaP-based nanocomposites, such as 3D printing scaffolds, oriented porous hydrogel, thin film coating, yet challenges exist.Additionally, more research is required to further disclose the inherent physical and chemical properties of GF-CaPs based biomaterials and to propose more tunable approaches in order to achieve nanostructured film coatings and to build hierarchical porous sprays. On the other hand, extra potential applications for this GF-based CaP coated hybrid architectures ought to be revealed. Many applications are still restricted to bone recovery. Recent advancements have shown that electrically conductive and mechanical properties endow GF-CaP-based composites with a promising potential for bone tissue engineering. GF-CaP coatings large surface area confers them the ability as carriers to concentrate growing factors and many other kinds of ECM proteins to uphold cell adhesion, thus succeeding the cells' existence and proliferation in stem cell therapy in bone research. The GF-CaP hybrid architectures have been attained in dissimilar 2D and 3D forms, like micro/nanofabrication, multilayer coating and free-standing films, and even 3D foams. These materials have revealed great potential for many applications instem cell and tissue engineerings. Both theextraordinary mechanical and electrical properties of GF-CaP coatings allow them to regulate stem cell growth anddifferentiation into aimed tissues, especially bone. Nevertheless, the underlying signaling pathways and mechanismsfor the differentiation and adhesion of stem cell on GF-CaP based substrates are yet not evidently understood. Additionally, studies are also needed to uncover the potential principles at the cellular/subcellular level and to offer new evidence for stem cell-based therapies. Besides, thedesign of GF-CaP hybrid substrates, 3D scaffolds or thin films,which have been interfaced with dissimilar nanomorphologies, mechanical and electrical stimulations, are both interesting and compulsory to further disclose the nanostructure−stem cellsinteractions.

Since GF-CaP is nonbiodegradable supplies, long-termand thorough histological studies of a broad range of organs and tissues will be significant to assess health risks,which is unsafe before these GF-CaPs can be used for implantable applications.More importantly, dissimilar aspects of the graphene based nanomaterials such as functionalization methods, and bioactivation of calcium phaosphate coatings and etc. were explained in detail. Also, numerous outstanding properties of the bioactive GF-CaPs and their research choices as well as the development potential and visions were discussed. Furthermore, this survey challenged the possibility of the graphene based scaffold surface that act as interesting signals for bone cells to promote the bone regeneration procedure.Nevertheless, along with detailed in vitro representation of scaffolds, more emphasis should be found on their evaluation in vivo with respect to inflammatory responses, regenerative potential and biocompatibility.

Acknowledgments: This work was supported by department of Plastic and Reconstructive Surgery, Craniofacial Research Center, Chang Gung memorial Hospital, Linkou, Taipei,Taiwan ROC. One of the authors, Dr.Manuri was sincerely grateful to the Professors H.T.Liao and J.P.Chen and Administrative office, School of Sciences, CTUAP, Vizianagaram, India.

References

1. H. Yi, F. Ur Rehman, C. Zhao, B. Liu and N. He, Recent advances in nano scaffolds for bone repair, Bone Res. 4 (2016) 16050.
2. J. Zheng, W. Xiao, Y. Fan, X. Xu, K. Zhang, D. Xie, R. Luo, X. Yang and B. Chen, Electro-deposited calcium phosphate compounds on graphene sheets: Blossoming flowers, Mater Lett. 179 (2016) 122-125.
3. Q. Wang, Y. Chu, J. He, W. Shao, Y. Zhou, K. Qi, L. Wang and S. Cui,A graded graphene oxide-hydroxyapatite/silk fibroin biomimetic scaffold for bone tissue engineering, Mater Sci Eng C Mater Biol Appl.80 (2017) 232-242.

 doi:10.20944/preprints202403.0428.v1

4. M. Li, Q. Liu, Z. Jia, X. Xu, Y. Cheng, Y. Zheng, T. Xi and S. Wei, Graphene oxide/hydroxyapatite composite coatings fabricated by electrophoretic nanotechnology for biological applications, Carbon. 67 (2014) 185-197.
5. M. Mehrali, E. Moghaddam, S. F. S. Shirazi, S. Baradaran, M. Mehrali, S. T. Latibari, H. S. C. Metselaar, N. A. Kadri, K. Zandi and N. A. A. Osman, Synthesis, Mechanical Properties, and in Vitro Biocompatibility with Osteoblasts of Calcium Silicate–Reduced Graphene Oxide Composites, ACS Appl Mater Interfaces.6 (2014) 3947-3962.
6. H. Liu, P. Xi, G. Xie, Y. Shi, F. Hou, L. Huang, F. Chen, Z. Zeng, C. Shao and J. Wang,Simultaneous Reduction and Surface Functionalization of Graphene Oxide for Hydroxyapatite Mineralization,J. Phys. Chem. C. 116 (2012) 3334-3341.
7. Y. Luo, H. Shen, Y. Fang, Y. Cao, J. Huang, M. Zhang, J. Dai, X. Shi and Z. Zhang, Enhanced Proliferation and Osteogenic Differentiation of Mesenchymal Stem Cells on Graphene Oxide-Incorporated Electrospun Poly(lactic-co-glycolic acid) Nanofibrous Mats,ACS Appl Mater Interfaces 7 (2015) 6331-6339.
8. Y. Talukdar, J. T. Rashkow, G. Lalwani, S. Kanakia and B. Sitharaman,The effects of graphene nanostructures on mesenchymal stem cells, Biomaterials.35 (2014) 4863-4877.
9. J.-W. Kim, Y. Shin, J.-J. Lee, E.-B. Bae, Y.-C. Jeon, C.-M. Jeong, M.-J. Yun, S.-H. Lee, D.-W. Han and J.-B. Huh,The Effect of Reduced Graphene Oxide-Coated Biphasic Calcium Phosphate Bone Graft Material on Osteogenesis,Int J Mol Sci.18 (2017) 1725.
10. J. H. Lee, Y. C. Shin, S.-M. Lee, O. S. Jin, S. H. Kang, S. W. Hong, C.-M. Jeong, J. B. Huh and D.-W. Han, Enhanced Osteogenesis by Reduced Graphene Oxide/Hydroxyapatite Nanocomposites, Sci Rep. 5 (2015)18833.
11. G. M. Neelgund, A. Oki and Z. Luo, In situ deposition of hydroxyapatite on graphene nanosheets, Mater Res Bull. 48 (2013) 175-179.
12. M. Li, Y. Wang, Q. Liu, Q. Li, Y. Cheng, Y. Zheng, T. Xi and S. Wei,In situ synthesis and biocompatibility of nano hydroxyapatite on pristine and chitosanfunctionalized graphene oxide,J. Mater Chem B. 1, (2013) 475-484.
13. V. Rosa, A. Della Bona, B. N. Cavalcanti and J. E. Nör,Tissue engineering: From research to dental clinics, Dent Mater, 28 (2012) 341-348.
14. P. Yu, R.-Y. Bao, X.-J. Shi, W. Yang and M.-B. Yang,Self-assembled high-strength hydroxyapatite/graphene oxide/chitosan composite hydrogel for bone tissue engineering,Carbohydr Polym.155 (2017) 507-515.
15. M. G. Raucci, D. Giugliano, A. Longo, S. Zeppetelli, G. Carotenuto and L. Ambrosio,Comparative facile methods for preparing graphene oxide–hydroxyapatite for bone tissue engineering,J Tissue Eng Regen Med.11 (2017) 2204-2216.
16. S. Bose, M. Roy and A. Bandyopadhyay,Recent advances in bone tissue engineering scaffolds,Trends Biotechno. 30 (2012) 546-554.
17. A. R. Amini, C. T. Laurencin and S. P. Nukavarapu, Bone tissue engineering: recent advances and challenges, Crit Rev Biomed Eng40 (2012) 363-408.
18. V. Rosa, T. M. Botero and J. E. Nör, Regenerative endodontics in light of the stem cell paradigm, Int Dent J.61 (2011) 23-28.
19. A. El-Fiqi, J. H. Lee, E.-J. Lee and H.-W. Kim, Collagen hydrogels incorporated with surface-aminated mesoporous nanobioactive glass: Improvement of physicochemical stability and mechanical properties is effective for hard tissue engineering, Acta Biomater. 9 (2013) 9508-9521.
20. X. Guan, M. Avci-Adali, E. Alarçin, H. Cheng, S. S. Kashaf, Y. Li, A. Chawla, H. L. Jang and A. Khademhosseini, Development of hydrogels for regenerative engineering, Biotechnol J. 12 (2017) 1600394-n/a.
21. C. Xie, H. Sun, K. Wang, W. Zheng, X. Lu and F. Ren, Graphene oxide nanolayers as nanoparticle anchors on biomaterial surfaces with nanostructures and charge balance for bone regeneration,J. Biomed Mater Res. A. 105 (2017) 1311-1323.
22. C. Wei, Z. Liu, F. Jiang, B. Zeng, M. Huang and D. Yu,Cellular behaviours of bone marrow-derived mesenchymal stem cells towards pristine graphene oxide nanosheets, Cell Proliferat.50 (2017) 1-10.
23. Y. Wang, X. Hu, J. Dai, J. Wang, Y. Tan, X. Yang, S. Yang, Q. Yuan and Y. Zhang,A 3D graphene coated bioglass scaffold for bone defect therapy based on the molecular targeting approach, J. Mater. Chem B.5 (2017) 6794-6800.
24. H. Ma, J. Chang and C. Wu, in Developments and Applications of Calcium Phosphate Bone Cements, eds. C. Liu and H. He, Springer Singapore, Singapore, 2018, DOI: 10.1007/978-981-10-5975-9_12, pp. 497-516.
25. H. D. Kim, J. Kim, R. H. Koh, J. Shim, J.-C. Lee, T.-I. Kim and N. S. Hwang,Enhanced Osteogenic Commitment of Human Mesenchymal Stem Cells on Polyethylene Glycol-Based Cryogel with Graphene Oxide Substrate, ACS Biomater Sci Eng. 3 (2017) 2470-2479.
26. P. Solis-Fernandez, M. Bissett and H. Ago, Synthesis, structure and applications of graphene-based 2D heterostructures, Chem Soc Rev, 46 (2017) 4572-4613.

 doi:10.20944/preprints202403.0428.v1

27. R. Al Faouri, R. Henry, A. S. Biris, R. Sleezer and G. J. Salamo,Adhesive force between graphene nanoscale flakes and living biological cells, J.Appl Toxicol. 37 (2017) 1346-1353.
28. S. Goenka, V. Sant and S. Sant, Graphene-based nanomaterials for drug delivery and tissue engineering, J. Control. Release. 173 (2014) 75-88.
29. G. Ersan, O. G. Apul, F. Perreault and T. Karanfil,Adsorption of organic contaminants by graphene nanosheets: A review,Water Res.126 (2017) 385-398.
30. G. Wang, B. Wang, J. Park, J. Yang, X. Shen and J. Yao, Synthesis of enhanced hydrophilic and hydrophobic graphene oxide nanosheets by a solvothermal method, Carbon47 (2009) 68-72.
31. Z. Lu, D. Hou, L. Meng, G. Sun, C. Lu and Z. Li,Mechanism of cement paste reinforced by graphene oxide/carbon nanotubes composites with enhanced mechanical properties,RSC Adv 5 (2015) 100598-100605.
32. Z. Pan, L. He, L. Qiu, A. H. Korayem, G. Li, J. W. Zhu, F. Collins, D. Li, W. H. Duan and M. C. Wang,Mechanical properties and microstructure of a graphene oxide-cement composite, Cement and Concrete Comp.58 (2015) 140-147.
33. Z. Lu, D. Hou, H. Ma, T. Fan and Z. Li, Effects of graphene oxide on the properties and microstructures of the magnesium potassium phosphate cement paste, Constr Build Mater. 119 (2016) 107-112.
34. J. H. Lee, Y. C. Shin, O. S. Jin, S. H. Kang, Y.-S. Hwang, J.-C. Park, S. W. Hong and D.-W. Han,Reduced graphene oxide-coated hydroxyapatite composites stimulate spontaneous osteogenic differentiation of human mesenchymal stem cells, Nanoscale. 7 (2015) 11642-11651.
35. R. Geetha Bai, N. Ninan, K. Muthoosamy and S. Manickam, Graphene: A versatile platform for nanotheranostics and tissue engineering, Prog. Mater. Sci. 91 (2018) 24-69.
36. S. Goenka, V. Sant and S. Sant, Graphene-based nanomaterials for drug delivery and tissue engineering, J. Control. Release. 173 (2014) 75-88.
37. E. Bressan, L. Ferroni, C. Gardin, L. Sbricoli, L. Gobbato, F. S. Ludovichetti, I. Tocco, A. Carraro, A. Piattelli and B. Zavan,Graphene based scaffolds effects on stem cells commitment, J. Transl Med. 12 (2014) 296.
38. B. S. Gomes, B. Simões and P. M. Mendes,The increasing dynamic, functional complexity of bio-interface materials, Nat. Rev Chem,2 (2018) 0120.
39. X.-B. Hu, Y.-L. Liu, W.-J. Wang, H.-W. Zhang, Y. Qin, S. Guo, X.-W. Zhang, L. Fu and W.-H. Huang, Biomimetic Graphene-Based 3D Scaffold for Long-Term Cell Culture and Real-Time Electrochemical Monitoring, Anal Chem.90 (2018) 1136-1141.
40. S. Yaragalla, M. A.P, N. Kalarikkal and S. Thomas, Chemistry associated with natural rubber–graphene nanocomposites and its effect on physical and structural properties, Ind Crops Prod. 74 (2015) 792-802.
41. D. Peizhen, S. Juan, Z. Guohong, X. Xu, J. Bo and Y. Jiaxin, Synthesis spherical porous hydroxyapatite/graphene oxide composites by ultrasonic-assisted method for biomedical applications,Biomed Mater. 13 (2018) 045001.
42. M. Li, P. Xiong, F. Yan, S. Li, C. Ren, Z. Yin, A. Li, H. Li, X. Ji, Y. Zheng and Y. Cheng,An overview of graphene-based hydroxyapatite composites for orthopedic applications, Bioactive Mater. 3 (2018) 1-18.
43. A. Moya, N. Larochette, M. Bourguignon, H. El-Hafci, E. Potier, H. Petite and D. Logeart-Avramoglou, Osteogenic potential of adipogenic predifferentiated human bone marrow-derived multipotent stromal cells for bone tissue-engineering,J. Tissue Eng Regen M. 12 (2018) e1511-e1524.
44. L. E. Bertassoni and M. V. Swain, Removal of dentin non-collagenous structures results in the unraveling of microfibril bundles in collagen type I,Connect Tissue Res. 2017, 58, 414-423.
45. R. Chakraborty, V. S. Seesala, M. Sen, S. Sengupta, S. Dhara, P. Saha, K. Das and S. Das, MWCNT reinforced bone like calcium phosphate—Hydroxyapatite composite coating developed through pulsed electrodeposition with varying amount of apatite phase and crystallinity to promote superior osteoconduction, cytocompatibility and corrosion protection performance compared to bare metallic implant surface, Surf Coat Tech. 325 (2017) 496-514.
46. C. Chen, X. Sun, W. Pan, Y. Hou, R. Liu, X. Jiang and L. Zhang,Graphene Oxide-Templated Synthesis of Hydroxyapatite Nanowhiskers To Improve the Mechanical and Osteoblastic Performance of Poly(lactic acid) for Bone Tissue Regeneration, ACS Sustain Chem Eng. 6 (2018) 3862-3869.
47. P. Hernigou,Authorities and foundation of the orthopaedic school in Germany in the 19th century: part II: Richard von Volkmann, Julius Wolff, Albert Hoffa, Friedrich Trendelenburg and other German authors.Int Orthop. 40 (2016) 843-853.
48. Y. Ikeda, T. Hasegawa, T. Yamamoto, P. H. L. de Freitas, K. Oda, A. Yamauchi and A. Yokoyama, Histochemical examination on the peri-implant bone with early occlusal loading after the immediate placement into extraction sockets,Histochem Cell Bio. 149 (2018) 433-447.
49. M. A. Hammond and J. M. Wallace,Exercise prevents β-aminopropionitrile-induced morphological changes to type I collagen in murine bone, BoneKEy Rep.4 (2015).
50. F. Hajiali, S. Tajbakhsh and A. Shojaei,Fabrication and Properties of Polycaprolactone Composites Containing Calcium Phosphate-Based Ceramics and Bioactive Glasses in Bone Tissue Engineering: A Review,Polym Rev. 58 (2018) 164-207.

51. V. Merk, M. Chanana, T. Keplinger, S. Gaan and I. Burgert, Hybrid wood materials with improved fire retardance by bio-inspired mineralisation on the nano- and submicron level,Green Chem. 17 (2015) 1423-1428.
52. A.-M. Pobloth, K. A. Johnson, H. Schell, N. Kolarczik, D. Wulsten, G. N. Duda and K. Schmidt-Bleek,Establishment of a preclinical ovine screening model for the investigation of bone tissue engineering strategies in cancellous and cortical bone defects, BMC Musculoskelet Disord. 17 (2016) 111.
53. R. W. Boyce, Q.-T. Niu and M. S. Ominsky, Kinetic reconstruction reveals time-dependent effects of romosozumab on bone formation and osteoblast function in vertebral cancellous and cortical bone in cynomolgus monkeys, Bone. 101 (2017) 77-87.
54. T. Omiya, J. Hirose, T. Hasegawa, N. Amizuka, Y. Omata, N. Izawa, H. Yasuda, Y. Kadono, M. Matsumoto, M. Nakamura, T. Miyamoto and S. Tanaka, The effect of switching from teriparatide to anti-RANKL antibody on cancellous and cortical bone in ovariectomized mice, Bone.107 (2018) 18-26.
55. H. Chirchir, T. L. Kivell, C. B. Ruff, J.-J. Hublin, K. J. Carlson, B. Zipfel and B. G. Richmond, Proc Natl Acad Sci U S A. 112 (2015) 366-371.
56. S. L. Manske, Y. Zhu, C. Sandino and S. K. Boyd,Human trabecular bone microarchitecture can be assessed independently of density with second generation HR-pQCT, Bone. 79 (2015) 213-221.
57. B. J. S. de Oliveira, L. C. Campanelli, D. P. Oliveira, A. P. de Bribean Guerra and C. Bolfarini, Surface characterization and fatigue performance of a chemical-etched Ti-6Al-4V femoral stem for cementless hip arthroplasty, Surf Coat Tech. 309 (2017) 1126-1134.
58. P. Ke, X.-N. Jiao, X.-H. Ge, W.-M. Xiao and B. Yu,From macro to micro: structural biomimetic materials by electrospinning,RSC Adv,4 (2014) 39704-39724.
59. W. D. HUA, P. P. CHEN, M. Q. XU, Z. AO, Y. LIU, D. HAN and F. HE,Quantitative description of collagen fibre network on trabecular bone surfaces based on AFM imaging, J. Microsc. 262 (2016) 112-122.
60. W. Shao, J. He, F. Sang, B. Ding, L. Chen, S. Cui, K. Li, Q. Han and W. Tan, Coaxial electrospun aligned tussah silk fibroin nanostructured fiber scaffolds embedded with hydroxyapatite–tussah silk fibroin nanoparticles for bone tissue engineering, Mater Sci Eng C Mater Biol Appl. 58 (2016) 342-351.
61. S. Wu, H. Zhai, W. Zhang and L. Wang, Monomeric Amelogenin's C-Terminus Modulates Biomineralization Dynamics of Calcium Phosphate, Cryst GrowthDes. 15 (2015) 4490-4497.
62. Q. Xie, Z. Xue, H. Gu, C. Hu, M. Yang, X. Wang and D. Xu, Molecular Dynamics Exploration of Ordered-to-Disordered Surface Structures of Biomimetic Hydroxyapatite Nanoparticles, J. Phys. Chem. C.122 (2018) 6691-6703.
63. S. Bsat, A. Speirs and X. Huang,Recent Trends in Newly Developed Plasma-Sprayed and Sintered Coatings for Implant Applications,J. Therm. Spray Technol. 25 (2016) 1088-1110.
64. T. A. Grünewald, H. Rennhofer, B. Hesse, M. Burghammer, S. E. Stanzl-Tschegg, M. Cotte, J. F. Löffler, A. M. Weinberg and H. C. Lichtenegger, Magnesium from bioresorbable implants: Distribution and impact on the nano- and mineral structure of bone, Biomaterials.76 (2016) 250-260.
65. M. Tanaka, A. Hosoya, H. Mori, R. Kayasuga, H. Nakamura and H. Ozawa,Minodronic acid induces morphological changes in osteoclasts at bone resorption sites and reaches a level required for antagonism of purinergic P2X2/3 receptors, J. Bone Miner Metab. 36 (2018) 54-63.
66. W. J. Basirun, B. Nasiri-Tabrizi and S. Baradaran, Overview of Hydroxyapatite–Graphene Nanoplatelets Composite as Bone Graft Substitute: Mechanical Behavior and In-vitroBiofunctionality,Crit Rev Solid State Mater Sci. 43 (2018) 177-212.
67. M. Albéric, A. Gourrier, W. Wagermaier, P. Fratzl and I. Reiche, The three-dimensional arrangement of the mineralized collagen fibers in elephant ivory and its relation to mechanical and optical properties, Acta Biomater.72 (2018) 342-351.
68. N. Mathavan, M. J. Turunen, M. Guizar-Sicairos, M. Bech, F. Schaff, M. Tägil and H. Isaksson,The compositional and nano-structural basis of fracture healing **in** healthy and osteoporotic bone,Sci Rep. 8 (2018) 1591.
69. Y. Wang and A. Ural, Mineralized collagen fibril network spatial arrangement influences cortical bone fracture behavior, J.Biomech. 66 (2018) 70-77.
70. Y. Wang and A. Ural,Effect of modifications in mineralized collagen fibril and extra-fibrillar matrix material properties on submicroscale mechanical behavior of cortical bone,J. Mech Behav Biomed Mater. 82 (2018) 18-26.
71. A. Hasan, V. Saxena and L. M. Pandey,Surface Functionalization of Ti6Al4V via Self-assembled Monolayers for Improved Protein Adsorption and Fibroblast Adhesion,Langmuir.34 (2018) 3494-3506.
72. C. Rey, C. Combes, C. Drouet, S. Cazalbou, D. Grossin, F. Brouillet and S. Sarda,Surface properties of biomimetic nanocrystalline apatites; applications in biomaterials,Prog. Cryst. Growth & Charact. 60 (2014)63-73.
73. A. D. Rafeek, G. Choi and L. A. Evans,Morphological, spectroscopic and crystallographic studies of calcium phosphate bioceramic powders, J. Aust Ceram Soc. 54 (2018) 161-168.

74. S. Tadier, S. Rokidi, C. Rey, C. Combes and P. G. Koutsoukos, Crystal growth of aragonite in the presence of phosphate, J. CrystGrowth.458 (2017) 44-52.
75. J. Yun, B. Holmes, A. Fok and Y. Wang, A Kinetic Model for Hydroxyapatite Precipitation in Mineralizing Solutions, Cryst. Growth Des.18 (2018) 2717–2725.
76. A. A. Poundarik, A. Boskey, C. Gundberg and D. Vashishth, Biomolecular regulation, composition and nanoarchitecture of bone mineral, Sci Rep.. 8 (2018) 1191.
77. L. Chen, R. Jacquet, E. Lowder and W. J. Landis,Refinement of collagen–mineral interaction: A possible role for osteocalcin in apatite crystal nucleation, growth and development, Bone. 71 (2015) 7-16.
78. J. Wang, G. Yang, Y. Wang, Y. Du, H. Liu, Y. Zhu, C. Mao and S. Zhang,Chimeric Protein Template-Induced Shape Control of Bone Mineral Nanoparticles and Its Impact on Mesenchymal Stem Cell Fate, Biomacromolecules. 16 (2015) 1987-1996.
79. J.M. Hughes, J.F. Rakovan,Structurally Robust, Chemically Diverse: Apatite and Apatite Supergroup Minerals,Elements. 11 (2015) 165-170.
80. J. M. D. A. Rollo, R. S. Boffa, R. Cesar, D. C. Schwab and T. P. Leivas,ssessment of Trabecular Bones Microarchitectures and Crystal Structure of Hydroxyapatite in Bone Osteoporosis with Application of the Rietveld Method,Procedia Eng. 110 (2015) 8-14.
81. H. Wu, D. Xu, M. Yang and X. Zhang,Surface Structure of Hydroxyapatite from Simulated Annealing Molecular Dynamics Simulations, Langmuir.32 (2016) 4643-4652.
82. M. B. Taşkın, Ö. Şahin, H. Taskin, O. Atakol, A. Inal and A. Gunes, Effect of synthetic nano-hydroxyapatite as an alternative phosphorus source on growth and phosphorus nutrition of lettuce (Lactuca sativa L.) plant, J. Plant Nutr.41 (2018) 1148-1154.
83. N. Eliaz and N. Metoki, Calcium Phosphate Bioceramics: A Review of Their History, Structure, Properties, Coating Technologies and Biomedical Applications, Materials.10 (2017) 334.
84. P. Bhanja, S. Chatterjee, A. K. Patra and A. Bhaumik, A new microporous oxyfluorinated titanium(IV) phosphate as an efficient heterogeneous catalyst for the selective oxidation of cyclohexanone, J. Colloid Interface Sci. 511 (2018) 92-100.
85. Z. B. Lai, R. Bai and C. Yan, Computational Materials Science.126 (2017) 59-65.
86. G. Ma and X. Y. Liu,Hydroxyapatite: Hexagonal or Monoclinic?, Cryst Growth Des. 9 (2009) 2991-2994.
87. K. Klimek, A. Przekora, A. Benko, W. Niemiec, M. Blazewicz and G. Ginalska, The use of calcium ions instead of heat treatment for β-1,3-glucan gelation improves biocompatibility of the β-1,3-glucan/HA bone scaffold, Carbohydr Polym.164 (2017) 170-178.
88. J.-P. Chen, M.-J. Tsai and H.-T. Liao,Incorporation of biphasic calcium phosphate microparticles in injectable thermoresponsive hydrogel modulates bone cell proliferation and differentiation,Colloids Surf B Biointerfaces. 110 (2013) 120-129.
89. R. Sammons,Hydroxyapatite (HAp) for Biomedical Applications, Woodhead Publishing sries in biomaterials. (2015) 53-83.
90. M. Vallet-Regí, D. A. Navarrete and D. Arcos, Biomimetic nanoceramics in clinical use: from materials to applications, Royal Society of Chemistry, 2008.
91. A. K. Nair, A. Gautieri, S.-W. Chang and M. J. Buehler, Molecular mechanics of mineralized collagen fibrils in bone, Nat Commun. (2013) 4 1724.
92. A. Masic, L. Bertinetti, R. Schuetz, S.-W. Chang, T. H. Metzger, M. J. Buehler and P. Fratzl, Osmotic pressure induced tensile forces in tendon collagen, Nat Commun.6 (2015) 5942.
93. M. J. Mirzaali, J. J. Schwiedrzik, S. Thaiwichai, J. P. Best, J. Michler, P. K. Zysset and U. Wolfram,Mechanical properties of cortical bone and their relationships with age, gender, composition and microindentation properties in the elderly, Bone. 93 (2016) 196-211.
94. S. C. Cox, J. A. Thornby, G. J. Gibbons, M. A. Williams and K. K. Mallick,3D printing of porous hydroxyapatite scaffolds intended for use in bone tissue engineering applications, Mater Sci Eng C Mater Biol Appl. 47 (2015) 237-247.
95. R.-M. Ion, D. Turcanu-Caruţiu, R.-C. Fierăscu, I. Fierăscu, I.-R. Bunghez, M.-L. Ion, S. Teodorescu, G. Vasilievici and V. Rădiţoiu,Caoxite-hydroxyapatite composition as consolidating material for the chalk stone from Basarabi–Murfatlar churches ensemble, Appl Surf Sci. 358 (2015) 612-618.
96. L. H. Tsung, J. I. B., M. K. G. and R. J. Peter, The Effects of Platelet-Rich Plasma on Cell Proliferation and Adipogenic Potential of Adipose-Derived Stem Cells,Tissue Eng A. 21 (2015) 2714-2722.
97. C.-Y. Kuo, C.-H. Chen, C.-Y. Hsiao and J.-P. Chen, Incorporation of chitosan in biomimetic gelatin/chondroitin-6-sulfate/hyaluronan cryogel for cartilage tissue engineering, Carbohydr Polym. 117 (2015) 722-730.
98. A. Niakan, S. Ramesh, P. Ganesan, C. Y. Tan, J. Purbolaksono, H. Chandran, S. Ramesh and W. D. Teng, Sintering behaviour of natural porous hydroxyapatite derived from bovine bone,Ceram. Int. 41 (2015) 3024-3029.

99. P. Gentile, C. Wilcock, C. Miller, R. Moorehead and P. Hatton, Process Optimisation to Control the Physico-Chemical Characteristics of Biomimetic Nanoscale Hydroxyapatites Prepared Using Wet Chemical Precipitation,Materials. 8 (2015) 2297-2310.
100. J. Zhang, W. Liu, O. Gauthier, S. Sourice, P. Pilet, G. Rethore, K. Khairoun, J.-M. Bouler, F. Tancret and P. Weiss, A simple and effective approach to prepare injectable macroporous calcium phosphate cement for bone repair: Syringe-foaming using a viscous hydrophilic polymeric solution, Acta Biomater.31 (2016) 326-338.
101. N. K. Nga, T. T. Hoai and P. H. Viet, Biomimetic scaffolds based on hydroxyapatite nanorod/poly(d,l) lactic acid with their corresponding apatite-forming capability and biocompatibility for bone-tissue engineering, Colloids Surf B Biointerfaces.128 (2015) 506-514.
102. S. Dhivya, S. Saravanan, T. P. Sastry and N. Selvamurugan, Nanohydroxyapatite-reinforced chitosan composite hydrogel for bone tissue repair in vitro and in vivo, J.Nanobiotechnol. 13 (2015) 40.
103. F. A. Shah, A. Snis, A. Matic, P. Thomsen and A. Palmquist,3D printed Ti6Al4V implant surface promotes bone maturation and retains a higher density of less aged osteocytes at the bone-implant interface,Acta Biomater. 30 (2016) 357-367.
104. V. Uskokovic, The role of hydroxyl channel in defining selected physicochemical peculiarities exhibited by hydroxyapatite,RSC Adv.5 (2015) 36614-36633.
105. R. Florencio-Silva, G. R. d. S. Sasso, E. Sasso-Cerri, M. J. Simoes and P. S. Cerri,Biology **of** bone tissue: structure, function, and factors that influence bone cells, BioMed res int., 2015, 2015.
106. Z. Li, J. Hardij, D. P. Bagchi, E. L. Scheller and O. A. MacDougald, Development, regulation, metabolism and function of bone marrow adipose tissues, Bone. 110 (2018) 134-140.
107. J. M. Bliley, W. N. Sivak, D. M. Minteer, C. Tompkins-Rhoades, J. Day, G. Williamson, H. T. Liao and K. G. Marra,Ethylene Oxide Sterilization Preserves Bioactivity and Attenuates Burst Release of Encapsulated Glial Cell Line Derived Neurotrophic Factor from Tissue Engineered Nerve Guides For Long Gap Peripheral Nerve Repair, ACS Biomater Sci Eng.1 (2015) 504-512.
108. J. T. Krawiec, H.-T. Liao, L. Kwan, A. D'Amore, J. S. Weinbaum, J. P. Rubin, W. R. Wagner and D. A. Vorp,Evaluation of the stromal vascular fraction of adipose tissue as the basis for a stem cell-based tissue-engineered vascular graft, J.Vasc Surg.66 (2017) 883-890.e881.
109. C.-M. Wu, Y.-A. Chen, H.-T. Liao, C.-h. Chen, C. H. Pan and C.-T. Chen,Surgical treatment of isolated zygomatic fracture: Outcome comparison between titanium plate and bioabsorbable plate, Asian J Sur.41 (2017) 370-376.
110. G.-J. Lai, K. T. Shalumon, S.-H. Chen and J.-P. Chen, Composite chitosan/silk fibroin nanofibers for modulation of osteogenic differentiation and proliferation of human mesenchymal stem cells, Carbohydr Polym. 111 (2014) 288-297.
111. J.-P. Chen and C.-H. Su, Surface modification of electrospun PLLA nanofibers by plasma treatment and cationized gelatin immobilization for cartilage tissue engineering, Acta Biomater. 7 (2011) 234-243.
112. E. Quinlan, A. López-Noriega, E. Thompson, H. M. Kelly, S. A. Cryan and F. J. O'Brien, Development of collagen–hydroxyapatite scaffolds incorporating PLGA and alginate microparticles for the controlled delivery of rhBMP-2 for bone tissue engineering, J. Control. Release.198 (2015) 71-79.
113. P.-Y. Chou, S.-H. Chen, C.-H. Chen, S.-H. Chen, Y. T. Fong and J.-P. Chen,Thermo-responsive in-situ forming hydrogels as barriers to prevent post-operative peritendinous adhesion,Acta Biomater. 63 (2017) 85-95.
114. M. D. Jones, P. S. Martin, J. M. Williams, A. M. Kemp and P. Theobald,Development of a computational biomechanical infant model for the investigation of infant head injury by shaking,Med. Sci. Law. 55 (2014) 291-299.
115. C. R. M. Black, V. Goriainov, D. Gibbs, J. Kanczler, R. S. Tare and R. O. C. Oreffo, Bone Tissue Engineering,Cur. Mol. Biol. Rep.1 (2015) 132-140.
116. X.Wang, S. Xu, S. Zhou, W. Xu, M.Leary, P.Choong, M. Qian, M. Brandt, Y.M.Xie.Extracellular matrix-based biomaterial scaffolds and the host response, Biomaterials,2016,83,127-141.
117. M. M. Stevens and J. H. George,Exploring and Engineering the Cell Surface Interface, Science. 310 (2005) 1135-1138.
118. H. Yu, B. Zhang, C. Bulin, R. Li and R. Xing, High-efficient Synthesis of Graphene Oxide Based on Improved Hummers Method, Sci Rep. 6 (2016) 36143.
119. C.-M. Seah, S.-P. Chai and A. R. Mohamed,Mechanisms of graphene growth by chemical vapour deposition on transition metals, Carbon 70 (2014) 1-21.
120. A. Janković, S. Eraković, M. Vukašinović-Sekulić, V. Mišković-Stanković, S. J. Park and K. Y. Rhee, Graphene-based antibacterial composite coatings electrodeposited on titanium for biomedical applications, Prog Org Coat. 83 (2015) 1-10.
121. S. Pina, J. M. Oliveira and R. L. Reis, Natural-based nanocomposites for bone tissue engineering and regenerative medicine: a review, Adv Mater.27 (2015)1143-1169.

 doi:10.20944/preprints202403.0428.v1

122. M. Brahmayya, S. A. Dai and S.-Y. Suen, Sulfonated reduced graphene oxide catalyzed cyclization of hydrazides and carbon dioxide to 1,3,4-oxadiazoles under sonication, Sci Rep. 7 (2017) 4675.
123. M. Brahmayya, S.-Y. Suen and S. A. Dai, Sulfonated graphene oxide-catalyzed N-acetylation of amines with acetonitrile under sonication, J Taiwan Inst Chem Eng. 2017.
124. S. Pei, Q. Wei, K. Huang, H.-M. Cheng and W. Ren, Green synthesis of graphene oxide by seconds timescale water electrolytic oxidation, Nat Commun. 9 (2018) 145.
125. M. Brahmayya and M.-L. Wang,Synthesis and Characterizations of Graphite Bisulphate and Its Selective Catalytic Activity in Presence of Cyclo Hexanone for the Acylation of Aromatic Compounds with the Carboxylic Acids under Ultrasound Irradiation, Int J Chem. 35 (2014) 1522-1530.
126. Z. Liu, Z. S. Wu, S. Yang, R. Dong, X. Feng and K. Müllen,Ultraflexible In-Plane Micro-Supercapacitors by Direct Printing of Solution-Processable Electrochemically Exfoliated Graphene, Adv Mater 28 (2016) 2217-2222.
127. S. Yang, M. R. Lohe, K. Mullen and X. Feng,New-Generation Graphene from Electrochemical Approaches: Production and Applications,Adv Mater 28 (2016) 6213-6221.
128. D. B. Shinde, J. Brenker, C. D. Easton, R. F. Tabor, A. Neild and M. Majumder,Shear Assisted Electrochemical Exfoliation of Graphite to Graphene, Langmuir.32 (2016) 3552-3559.
129. J.-Y. Choi, Graphene transfer: A stamp for all substrates, Nat nanotechnol.8 (2013) 311.
130. J. Song, F.-Y. Kam, R.-Q. Png, W.-L. Seah, J.-M. Zhuo, G.-K. Lim, P. K. Ho and L.-L. Chua, A general method for transferring graphene onto soft surfaces,Nat nanotechnol.8 (2013) 356-62.
131. P. Ruffieux, S. Wang, B. Yang, C. Sánchez-Sanchez, J. Liu, T. Dienel, L. Talirz, P. Shinde, C. A. Pignedoli and D. Passerone,On-surface synthesis of graphene nanoribbons with zigzag edge topology, Nature.531 (2016) 489-492.
132. Y.-Z. Tan, B. Yang, K. Parvez, A. Narita, S. Osella, D. Beljonne, X. Feng and K. Müllen,Atomically precise edge chlorination of nanographenes and its application in graphene nanoribbons, Nat commun..4 (2013) 2646.
133. K.-I. Choi, T.-H. Kim, Y. Lee, H. Kim, H. Lee, G. Yuan, S. K. Satija, J. H. Choi, H. Ahn and J. Koo, Perpendicular Orientation of Diblock Copolymers Induced by Confinement between Graphene Oxide Sheets, Langmuir.34 (2018)1681–1690.
134. J. Kim, L. J. Cote, F. Kim, W. Yuan, K. R. Shull and J. Huang, Graphene Oxide Sheets at Interfaces, J.Am Chem Soc.132 (2010) 8180-8186.
135. M. Khandelwal, Y. Li, S. H. Hur and J. S. Chung,Surface modification of co-doped reduced graphene oxide through alkanolamine functionalization for enhanced electrochemical performance, New J Chem.42 (2018) 1105-1114.
136. G. S., B. A., S. T. and D. N., Molecular sensitivity of metal nanoparticles decorated graphene-family nanomaterials as surface-enhanced Raman scattering (SERS) platforms,J. Raman Spectrosc..49 (2018) 438-451.
137. L. Dong, J. Yang, M. Chhowalla and K. P. Loh, Synthesis and reduction of large sized graphene oxide sheets. Chem Soc Rev. 46 (2017) 7306-7316.
138. H. Zhao, W. Dong, Y. Zheng, A. Liu, J. Yao, C. Li, W. Tang, B. Chen, G. Wang and Z. Shi,The structural and biological properties of hydroxyapatite-modified titanate nanowire scaffolds, Biomaterials 32 (2011) 5837-5846.
139. C. Fu, B. Song, C. Wan, K. Savino, Y. Wang, X. Zhang and M. Z. Yates,Electrochemical growth of composite hydroxyapatite coatings for controlled release,Surf Coat Tech. 276 (2015) 618-625.
140. Y. Zeng, X. Pei, S. Yang, H. Qin, H. Cai, S. Hu, L. Sui, Q. Wan and J. Wang, Graphene oxide/hydroxyapatite composite coatings fabricated by electrochemical deposition, Surf Coat Tech.286 (2016) 72-79.
141. Y. W. Gu, N. H. Loh, K. A. Khor, S. B. Tor and P. Cheang, Spark plasma sintering of hydroxyapatite powders, Biomaterials. 23 (2002) 37-43.
142. S. Klébert, C. Balázsi, K. Balázsi, E. Bódis, P. Fazekas, A. M. Keszler, J. Szépvölgyi and Z. Károly,Spark plasma sintering of graphene reinforced hydroxyapatite composites,Ceram. Int.41 (2015) 3647-3652.
143. I. Bajpai, D.-Y. Kim, Y.-H. Han, B.-K. Jang and S. Kim, Directional property evaluation of spark plasma sintered GNPs-reinforced hydroxyapatite composites, Mater Lett. 158 (2015) 62-65.
144. L. Zhang, W. Liu, C. Yue, T. Zhang, P. Li, Z. Xing and Y. Chen, A tough graphene nanosheet/hydroxyapatite composite with improved in vitrobiocompatibility, Carbon. 61 (2013) 105-115.
145. A. Repanas, S. Andriopoulou and B. Glasmacher,The significance of electrospinning as a method to create fibrous scaffolds for biomedical engineering and drug delivery applications, J. Drug Deliv Sci Tec31 (2016) 137-146.
146. H. Ma, W. Su, Z. Tai, D. Sun, X. Yan, B. Liu and Q. Xue, Preparation and cytocompatibility of polylactic acid/hydroxyapatite/graphene oxide nanocomposite fibrous membrane, Chin Sci Bull. 57 (2012) 3051-3058.
147. Y. Liu, J. Huang and H. Li,Synthesis of hydroxyapatite–reduced graphite oxide nanocomposites for biomedical applications: oriented nucleation and epitaxial growth of hydroxyapatite,J Mater Chem B. 1 (2013) 1826-1834.

 doi:10.20944/preprints202403.0428.v1

148. W. Nie, C. Peng, X. Zhou, L. Chen, W. Wang, Y. Zhang, P. X. Ma and C. He,Three-dimensional porous scaffold by self-assembly of reduced graphene oxide and nano-hydroxyapatite composites for bone tissue engineering, Carbon, 116 (2017) 325-337.
149. C. C. Berndt, F. Hasan, U. Tietz and K.-P. Schmitz, Advances in Calcium Phosphate Biomaterials.2 (2014)267-329.
150. Y. Liu, Z. Dang, Y. Wang, J. Huang and H. Li, Hydroxyapatite/graphene-nanosheet composite coatings deposited by vacuum cold spraying for biomedical applications: Inherited nanostructures and enhanced properties, Carbon. 67 (2014) 250-259.
151. S. Bose, S. Vahabzadeh and A. Bandyopadhyay,Bone tissue engineering using 3D printing, Mater Today. 16 (2013) 496-504.
152. C. Wu, L. Xia, P. Han, M. Xu, B. Fang, J. Wang, J. Chang and Y. Xiao, Graphene-oxide-modified β-tricalcium phosphate bioceramics stimulate in vitro and in vivo osteogenesis, Carbon. 93 (2015) 116-129.
153. Y. Zhang, L. Zhang and C. Zhou, Review of Chemical Vapor Deposition of Graphene and Related Applications,Acc Chem Res.46 (2013) 2329-2339.
154. A. R. Biris, M. Mahmood, M. D. Lazar, E. Dervishi, F. Watanabe, T. Mustafa, G. Baciut, M. Baciut, S. Bran, S. Ali and A. S. Biris, Novel Multicomponent and Biocompatible Nanocomposite Materials Based on Few-Layer Graphenes Synthesized on a Gold/Hydroxyapatite Catalytic System with Applications in Bone Regeneration,J. Phys. Chem. C. 115 (2011) 18967-18976.
155. L. Boilet, M. Descamps, E. Rguiti, A. Tricoteaux, J. Lu, F. Petit, V. Lardot, F. Cambier and A. Leriche,Processing and properties of transparent hydroxyapatite and β tricalcium phosphate obtained by HIP process,Ceram. Int. 39 (2013) 283-288.
156. S. Baradaran, E. Moghaddam, B. Nasiri-Tabrizi, W. J. Basirun, M. Mehrali, M. Sookhakian, M. Hamdi and Y. Alias,Characterization of nickel-doped biphasic calcium phosphate/graphene nanoplatelet composites for biomedical application, Mater Sci Eng C Mater Biol Appl. 49 (2015) 656-668.
157. Y. Zhao, K.-N. Sun, W.-L. Wang, Y.-X. Wang, X.-L. Sun, Y.-J. Liang, X.-N. Sun and P.-F. Chui, Microstructure and anisotropic mechanical properties of graphene nanoplatelet toughened biphasic calcium phosphate composite, Ceram. Int.39 (2013) 7627-7634.
158. S. Baradaran, E. Moghaddam, W. J. Basirun, M. Mehrali, M. Sookhakian, M. Hamdi, M. R. N. Moghaddam and Y. Alias, Mechanical properties and biomedical applications of a nanotube hydroxyapatite-reduced graphene oxide composite, Carbon. 69 (2014) 32-45.
159. F. Gao, C. Xu, H. Hu, Q. Wang, Y. Gao, H. Chen, Q. Guo, D. Chen and D. Eder, Biomimetic synthesis and characterization of hydroxyapatite/graphene oxide hybrid coating on Mg alloy with enhanced corrosion resistance, Mater Lett. 138 (2015) 25-28.
160. H. Liu, J. Cheng, F. Chen, D. Bai, C. Shao, J. Wang, P. Xi and Z. Zeng, Gelatin functionalized graphene oxide for mineralization of hydroxyapatite: biomimetic and in vitro evaluation,Nanoscale.6 (2014) 5315-5322.
161. H. Peng, L. Meng, L. Niu and Q. Lu,Simultaneous Reduction and Surface Functionalization of Graphene Oxide by Natural Cellulose with the Assistance of the Ionic Liquid, J. Phys. Chem. C. 116 (2012) 16294-16299.
162. H. Liu, J. Cheng, F. Chen, F. Hou, D. Bai, P. Xi and Z. Zeng, Biomimetic and Cell-Mediated Mineralization of Hydroxyapatite by Carrageenan Functionalized Graphene Oxide, ACS Appl Mater Interfaces.6 (2014) 3132-3140.
163. C. Xie, X. Lu, L. Han, J. Xu, Z. Wang, L. Jiang, K. Wang, H. Zhang, F. Ren and Y. Tang,Biomimetic Mineralized Hierarchical Graphene Oxide/Chitosan Scaffolds with Adsorbability for Immobilization of Nanoparticles for Biomedical Applications,ACS Appl Mater Interfaces. 8 (2016) 1707-1717.
164. D. Depan, T. C. Pesacreta and R. D. K. Misra, The synergistic effect of a hybrid graphene oxide–chitosan system and biomimetic mineralization on osteoblast functions, Biomater Sci. 2 (2014) 264-274.
165. J. Wang, H. Wang, Y. Wang, J. Li, Z. Su and G. Wei, Alternate layer-by-layer assembly of graphene oxide nanosheets and fibrinogen nanofibers on a silicon substrate for a biomimetic three-dimensional hydroxyapatite scaffold,J Mater Chem B, 2 (2014) 7360-7368.
166. A. Ashkan, J. A. H. and J. A. C.,The effect of graphene substrate on osteoblast cell adhesion and proliferation, J Biomed Mater Res A.102 (2014) 3282-3290.
167. R. Tatavarty, H. Ding, G. Lu, R. J. Taylor and X. Bi, Synergistic acceleration in the osteogenesis of human mesenchymal stem cells by graphene oxide–calcium phosphate nanocomposites,Chem Commun. 50 (2014) 8484-8487.
168. S. Wang, S. Zhang, Y. Wang, X. Sun and K. Sun, Reduced graphene oxide/carbon nanotubes reinforced calcium phosphate cement, Ceram. Int. 43 (2017) 13083-13088.
169. Y. C. Shin, J. H. Lee, O. S. Jin, S. H. Kang, S. W. Hong, B. Kim, J.-C. Park and D.-W. Han, Synergistic effects of reduced graphene oxide and hydroxyapatite on osteogenic differentiation of MC3T3-E1 preosteoblasts,Carbon. 95 (2015) 1051-1060.

170. N. Manitha, D. Nancy, G. K. Amit, G. S. Anjusree, V. Sajini and V. N. Shantikumar,Graphene oxide nanoflakes incorporated gelatin–hydroxyapatite scaffolds enhance osteogenic differentiation of human mesenchymal stem cells, Nanotechnol. 26 (2015) 161001.
171. Q. Zhang, Y. Liu, Y. Zhang, H. Li, Y. Tan, L. Luo, J. Duan, K. Li and C. E. Banks,Facile and controllable synthesis of hydroxyapatite/graphene hybrid materials with enhanced sensing performance towards ammonia, Analyst. 140 (2015) 5235-5242.
172. X. Xie, K. Hu, D. Fang, L. Shang, S. D. Tran and M. Cerruti,Graphene and hydroxyapatite self-assemble into homogeneous, free standing nanocomposite hydrogels for bone tissue engineering, Nanoscale. 7 (2015) 7992-8002.
173. C. Wu, P. Han, X. Liu, M. Xu, T. Tian, J. Chang and Y. Xiao, Mussel-inspired bioceramics with self-assembled Ca-P/polydopamine composite nanolayer: Preparation, formation mechanism, improved cellular bioactivity and osteogenic differentiation of bone marrow stromal cells, Acta Biomater.10 (2014) 428-438.
174. M. Gu, Y. Liu, T. Chen, F. Du, X. Zhao, C. Xiong and Y. Zhou, Is Graphene a Promising Nano-Material for Promoting Surface Modification of Implants or Scaffold Materials in Bone Tissue Engineering ?, Tissue Eng B: Reviews.20 (2014) 477-491.
175. A. M. Monaco and M. Giugliano,Carbon-based smart nanomaterials in biomedicine and neuroengineering,Beilstein J. Nanotechnol.5 (2014) 1849-1863.
176. Z. Huang, S. Guan, Y. Wang, G. Shi, L. Cao, Y. Gao, Z. Dong, J. Xu, Q. Luo and J. Liu,Self-assembly of amphiphilic peptides into bio-functionalized nanotubes: a novel hydrolase model, J Mater Chem B. 1(2013) 2297-2304.
177. J. Swift, I. L. Ivanovska, A. Buxboim, T. Harada, P. C. D. P. Dingal, J. Pinter, J. D. Pajerowski, K. R. Spinler, J.-W. Shin, M. Tewari, F. Rehfeldt, D. W. Speicher and D. E. Discher, Nuclear lamin-A scales with tissue stiffness and enhances matrix-directed differentiation,Science.(2013) 341.
178. N. Dubey, R. Bentini, I. Islam, T. Cao, A. H. Castro Neto and V. Rosa, Graphene: A Versatile Carbon-Based Material for Bone Tissue Engineering, Stem Cells Int. 2015, (2015) 12.
179. K. Sungjin, K. S. Hee, L. S. Yoon, K. J. Hong and P. C. Beum, Graphene–Biomineral Hybrid Materials, Adv Mater. 23 (2011) 2009-2014.
180. Y. Liu, J. Huang and H. Li,Nanostructural Characteristics of Vacuum Cold-Sprayed Hydroxyapatite/GrapheneNanosheet Coatings for Biomedical Applications,**J**. Therm. Spray Technol. 23 (2014) 1149-1156.
181. C. He, Z.-Q. Shi, C. Cheng, H.-Q. Lu, M. Zhou, S.-D. Sun and C.-S. Zhao, Graphene oxide and sulfonated polyanion co-doped hydrogel films for dual-layered membranes with superior hemocompatibility and antibacterial activity, Biomater sci.4 (2016) 1431-1440.
182. C. He, C. Cheng, S.-Q. Nie, L.-R. Wang, C.-X. Nie, S.-D. Sun and C.-S. Zhao,Graphene oxide linked sulfonate-based polyanionic nanogels as biocompatible, robust and versatile modifiers of ultrafiltration membranes, JMater Chem B.4 (2016) 6143-6153.
183. S. H. Ku, M. Lee and C. B. Park,Carbon-Based Nanomaterials for Tissue Engineering, Adv healthcare mater. 2 (2103) 244-260.
184. L. W. Cheng, L. C. Haley, Kenry, S. Chenliang, L. K. Ping and L. C. Teck, Cell-assembled graphene biocomposite for enhanced chondrogenic differentiation,Small, 2015, 11, 963-969.
185. T. R. Nayak, H. Andersen, V. S. Makam, C. Khaw, S. Bae, X. Xu, P.-L. R. Ee, J.-H. Ahn, B. H. Hong, G. Pastorin and B. Özyilmaz, Graphene for Controlled and Accelerated Osteogenic Differentiation of Human Mesenchymal Stem Cells, ACS Nano.5 (2011) 4670-4678.
186. Q. Tu, L. Pang, Y. Chen, Y. Zhang, R. Zhang, B. Lu and J. Wang,Effects of surface charges of graphene oxide on neuronal outgrowth and branching, Analyst. 139 (2014) 105-115.
187. T. L. A. L., L. W. Cheng, S. Hui, W. E. Y. L., S. Anton, G. Sergey, H. Jonathan, L. C. Teck and L. K. Ping,Highly Wrinkled Cross-Linked Graphene Oxide Membranes for Biological and Charge-Storage Applications, Small. 8 (2012) 423-431.
188. M. J. Dalby, N. Gadegaard and R. O. C. Oreffo, Harnessing nanotopography and integrin–matrix interactions to influence stem cell fate, Nat Mater.13 (2014) 558-569.
189. D. A. Dikin, S. Stankovich, E. J. Zimney, R. D. Piner, G. H. B. Dommett, G. Evmenenko, S. T. Nguyen and R. S. Ruoff,Preparation and characterization of graphene oxide paper, Nature.448 (2007) 457-460.
190. J. K. Wang, G. M. Xiong, M. Zhu, B. Ozyilmaz, A. H. Castro Neto, N. S. Tan and C. Choong, Polymer-Enriched 3D Graphene Foams for Biomedical Applications**,** ACS Appl Mater Interfaces.7 (2015) 8275-8283.
191. T. Maiyalagan, X. Dong, P. Chen and X. Wang, Electrodeposited Pt on three-dimensional interconnected graphene as a free-standing electrode for fuel cell application,J Mater Chem. 22 (2012) 5286-5290.
192. J. Park, H. Park, P. Ercius, A. F. Pegoraro, C. Xu, J. W. Kim, S. H. Han and D. A. Weitz, Direct Observation of Wet Biological Samples by Graphene Liquid Cell Transmission Electron Microscopy,Nano Lett.15 (2015) 4737-4744.

 doi:10.20944/preprints202403.0428.v1

193. T. D. Y. Kozai, N. B. Langhals, P. R. Patel, X. Deng, H. Zhang, K. L. Smith, J. Lahann, N. A. Kotov and D. R. Kipke, Ultrasmall implantable composite microelectrodes with bioactive surfaces for chronic neural interfaces, Nat mater.11 (2012) 1065.
194. N. A. Kotov, J. O. Winter, I. P. Clements, E. Jan, B. P. Timko, S. Campidelli, S. Pathak, A. Mazzatenta, C. M. Lieber and M. Prato, Nanomaterials for Neural Interfaces, Adv Mater. 21 (2009) 3970-4004.
195. I. R. Minev, P. Musienko, A. Hirsch, Q. Barraud, N. Wenger, E. M. Moraud, J. Gandar, M. Capogrosso, T. Milekovic, L. Asboth, R. F. Torres, N. Vachicouras, Q. Liu, N. Pavlova, S. Duis, A. Larmagnac, J. Vörös, S. Micera, Z. Suo, G. Courtine and S. P. Lacour, Electronic dura mater for long-term multimodal neural interfaces, Science. 347 (2015) 159-163.
196. M. Li, P. Xiong, F. Yan, S. Li, C. Ren, Z. Yin, A. Li, H. Li, X. Ji and Y. Zheng,An overview of graphene-based hydroxyapatite composites for orthopedic applications, Bioactive mater. 3 (2018) 1-18.
197. L. H. Hess, M. Seifert and J. A. Garrido, Graphene Transistors for Bioelectronics,Proc IEEE, 101 (2013) 1780-1792.
198. R. Podila, T. Moore, F. Alexis and A. M. Rao, Graphene coatings for enhanced hemo-compatibility of nitinol stents, RSC Adv. 3 (2013) 1660-1665.
199. X. Liu, Y. Cao, M. Zhao, J. Deng, X. Li and D. Li, The enhanced anticoagulation for graphene induced by $COOH^+$ ion implantation, Nanoscale res lett. 10 (2015) 14.
200. S. Gurunathan and J.-H. Kim, Synthesis, toxicity, biocompatibility, and biomedical applications of graphene and graphene-related materials,Int J Nanomed.11 (2016) 1927-1945.
201. Y. Yan, X. Zhang, H. Mao, Y. Huang, Q. Ding and X. Pang, Hydroxyapatite/gelatin functionalized graphene oxide composite coatings deposited on TiO_2 nanotube by electrochemical deposition for biomedical applications, Appl Surf Sci. 329 (2015) 76-82.
202. Y. Shi, M. Li, Q. Liu, Z. Jia, X. Xu, Y. Cheng and Y. Zheng,Electrophoretic deposition of graphene oxide reinforced chitosan–hydroxyapatite nanocomposite coatings on Ti substrate, J Mater Sc: Mater Med. 27 (2016) 48.
203. Weibo Xie, Fuxiang Song, Rui Wang, Shenglin Sun, Miao Li, Zengjie Fan, Bin Liu, Qiangqiang Zhang, JizengWang,Mechanically Robust 3D Graphene-Hydroxyapatite Hybrid Bioscaffolds with Enhanced Osteoconductive and Biocompatible Performance,Crystals, 2018, 105, 1-12.
204. Q.Zhang; B. Zhang,Y.Yu, K.Zhao,P. He, B.Huang. Fluoroalkyl-silane-modified 3D graphene foam with improved Joule-heating effects and high hydrophobicity-derived anti-icing properties. J. Mater. Sci. 2018, 53, 528–537.